Design, Synthesis, and Biological Evaluation of a Series of 2-Hydroxyisoquinoline-1,3(2*H*,4*H*)-diones as Dual Inhibitors of Human Immunodeficiency Virus Type 1 Integrase and the Reverse Transcriptase RNase H Domain

Muriel Billamboz,[†] Fabrice Bailly,*[,†] Maria Letizia Barreca,[‡] Laura De Luca,[§] Jean-François Mouscadet,[||] Christina Calmels,[⊥] Marie-Line Andréola,[⊥] Myriam Witvrouw,[@] Frauke Christ,[@] Zeger Debyser,[@] and Philippe Cotelle[†]

Laboratoire de Chimie Organique et Macromoléculaire, UMR CNRS 8009, Université de Lille 1, 59655 Villeneuve d'Ascq, France, Dipartimento di Chimica e Tecnologia del farmaco, Sezione di Chimica Farmaceutica II, Universita di Perugia, Via del Liceo 1, 06123 Perugia, Italy, Dipartimento Farmaco-Chimico, Universita di Messina, Viale Annunziata, 98168 Messina, Italy, Laboratoire de Biotechnologies et Pharmacologie Génétique Appliquée, UMR CNRS 8113, Ecole Normale Supérieure de Cachan, 61 av du Président Wilson, 94235 Cachan, France, Institut Fédératif de Recherches "Pathologies Infectieuses et Cancers" (IFR 66), MCMP-UMR 5234 CNRS, Université Victor Segalen Bordeaux 2, 33076 Bordeaux, France, and Molecular Medicine, K. U. Leuven and IRC KULAK, Kapucijnenvoer 33, B-3000 Leuven, Flanders, Belgium

Received June 12, 2008

We report herein the synthesis of a series of 19 2-hydroxyisoquinoline-1,3(2*H*,4*H*)-dione derivatives variously substituted at position 7 aimed at inhibiting selectively two-metal ion catalytic active sites. The compounds were tested against HIV-1 reverse transcriptase (RT) polymerase, HIV-1 RT ribonuclease H (RNase H), and HIV-1 integrase (IN). Most compounds displayed poor inhibition of RT polymerase even at 50 μM. The majority of the synthesized compounds inhibited RNase H and IN at micromolar concentrations, and some of them were weakly selective for IN. Surprisingly, two new hits were discovered, which displayed a high selectivity for IN with submicromolar IC_{50} values. These enzymatic inhibitory properties may be related to the metal binding abilities of the compounds. Physicochemical studies were consistent with a 1/1 stoichiometry of the magnesium complexes in solution, and the metal complexation was strictly dependent on the enolization abilities of the compounds. Unfortunately, all tested compounds exhibited high cellular cytotoxicity in cell culture which limits their applications as antiviral agents.

Introduction

Human immunodeficiency virus type 1 (HIV-1)[a] integrase (IN) is an essential enzyme for viral replication and mediates the insertion of viral DNA within the host cell genome via a multistep process that occurs in discrete biochemical stages: (i) assembly of a stable DNA−enzyme complex with specific DNA sequences at the end of the HIV-1 long terminal repeat (LTR) regions, (ii) endonucleolytic process of the viral DNA removing the terminal dinucleotide from each 3′-end (3′-processing), (iii) strand transfer in which the viral DNA 3′-ends are covalently linked to the cellular DNA, (iv) removal of the two unpaired nucleotides at the 3′-ends of the viral DNA, and (v) gap filling, probably accomplished by cellular enzymes. In the past decade, IN has emerged as an attractive target because it is necessary for stable infection and there is no known mammalian homologue of IN. The IN catalytic domain contains a triad of invariant carboxylate residues, D64, D116, and E152 (the so-called DDE motif), which are required for catalysis. The Mg^{2+} ion is coordinated by D64 and D116 along with water molecules, whereas E152 that lies close to D64 does not participate in metal binding.[1,2] Whereas structural studies of IN reveal a single binding site for Mg^{2+}, the number of metal ions present and required in the active site during the process remains controversial.

A great number of HIV-1 integrase inhibitors with metal binding properties have been described, and numerous reviews have been published.[3−9] Two IN inhibitors, GS-9137 (Elvitegravir)[10] and MK-0518 (Raltegravir),[11,12] demonstrated promising clinical trial results and advanced into later stage trials, the latter being the first U.S. FDA-approved drug targeting IN.

Reverse transcriptase (RT) is another important HIV-1 enzyme that led to the design of numerous anti-HIV drugs. This multifunctional enzyme has RNA- and DNA-dependent DNA polymerase, strand displacement, strand transfer, and RNase H activities.[13,14] RNase H activity, which degrades RNA in RNA−DNA hybrid molecules, is required at several steps during the reverse transcription process, and a functional ribonuclease H (RNase H) is essential for retroviral replication. The crystal and NMR structures of the isolated HIV RNase H domain are similar to the structure of the RNase H domain as part of the full-length HIV-RT protein.[15,16] HIV IN and RNase H belong to a broader class of nucleotide-related enzymes including nucleases, polymerases, and polynucleotidyl transferases.[17] Determination of the three-dimensional structures of the catalytic core of HIV-1 RNase H led to the surprising finding that HIV-1 RNase H and HIV-1 IN are folded in a very similar way and have comparable active site geometries. Both HIV-1 RNase H and IN catalytic cores share a similar $\alpha\beta$-fold containing a central five-stranded mixed β-sheet surrounded by α-helices on both sides, which are in the same topological order.[18−20] These

* To whom correspondence should be addressed. Telephone: +33 320 33 72 31. Fax: +33 320 33 63 09. E-mail: fabrice.bailly@univ-lille1.fr.
[†] Université de Lille 1.
[‡] Universita di Perugia.
[§] Universita di Messina.
[||] Ecole Normale Supérieure de Cachan.
[⊥] Université Victor Segalen Bordeaux 2.
[@] K. U. Leuven and IRC KULAK.

[a] Abbreviations: HIV-1, human immunodeficiency virus type 1; IN, integrase; LTR, long terminal repeat; RT, reverse transcriptase; RNase H, ribonuclease H; 3′-P, 3′-processing; ST, strand transfer; MTT, 3-(4,5-dimethylthiazol-2-yl)-2,5-diphenyltetrazolium bromide; DKA, β-diketo acid; HBA, hydrogen bond acceptor; HBD, hydrogen bond donor; HY Ar, hydrophobic aromatic; DTT, dithiothreitol; HEPES, 4-(2-hydroxyethyl)piperazine-1-ethanesulfonic acid; PEG, polyethylene glycol; CPE, cytopathic effect.

10.1021/jm8007085 CCC: $40.75
Published on Web 11/21/2008

Scheme 1. Synthesis of Compounds **6a**−**g**[a]

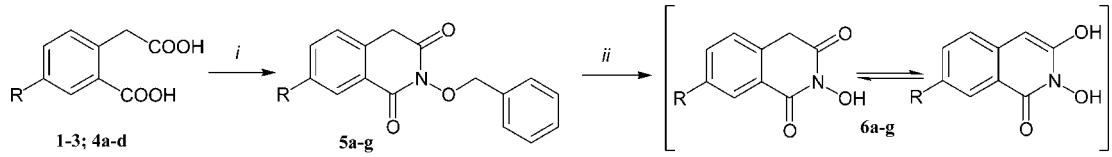

[a] Reagents and conditions: (i) 1.2 equiv of NH_2OBn, toluene, Dean−Stark apparatus, reflux, 12 h; (ii) BBr_3, 4.0 equiv, room temperature, 1 h; H_2O, room temperature, 15 min.

enzymes have remarkably similar active sites with the same DDE triad absolutely required for catalytic activity. The number of metal divalent ions involved in catalysis is still subject to debate for both enzymes. Similar structural features comprising three aspartate residues and two magnesium ions separated by 3.57 Å were evidenced for the polymerase active site of RT in complex with a primer−template DNA duplex and an incoming nucleotide.[16,21,22]

Some diketo acid inhibitors of HIV-1 IN have shown anti-RNase H activities,[23,24] whereas DNA aptamers first described as inhibitors of RNase H have been reported to inhibit HIV-1 integrase.[25] Recently, tropolones[26−28] and madurahydroxylactone derivatives[29] have been reported to inhibit both enzymes. Thus, the simultaneous inhibition of HIV-1 IN, RT polymerase, and RT RNase H activities by metal-chelating compounds appears as a novel and attractive therapeutic way which could overcome the problems occurring during combination therapy.

2-Hydroxyisoquinoline-1,3(2*H*,4*H*)-dione was reported as a selective RT RNase H versus polymerase inhibitor.[30] Indeed, RNA-dependent DNA polymerase was inhibited with an IC_{50} of 40 μM, in comparison with RNase activity which is inhibited with an IC_{50} of ≤ 1 μM. This compound, termed *N*-hydroxyimide, was previously designed as a targeted active site binding inhibitor with selectivity for two-metal ion enzymes[31] and was shown to inhibit the activity of the isolated RT RNase H domain as well as the RNase H activity of full-length HIV-1 RT based on its supposed capacities to bind to this isolated domain.[32] 2-Hydroxyisoquinoline-1,3(2*H*,4*H*)-dione is the prototype compound of a series of *N*-hydroxyimides for which three oxygen atoms present optimal distances for interaction with two divalent metal ions bound at a distance of 4−5 Å in the RT RNase H and IN active sites. We considered 2-hydroxyisoquinoline-1,3(2*H*,4*H*)-dione as a potential lead compound for the development of novel dual IN/RNase H inhibitors.

Here we report the synthesis and comparative evaluation of a series of 2-hydroxyisoquinoline-1,3(2*H*,4*H*)-dione derivatives variously substituted at position 7 as inhibitors of HIV-1 IN, HIV-1 RT polymerase, and HIV-1 RT RNase H. The structural requirements for the inhibition of integrase versus RNase H are discussed. The antiviral activities were also evaluated. Finally, we investigated the ability of these compounds to interact with metallic divalent cations as previously stated.

Results and Discussion

Chemistry. The main previously reported method of creating the 2-hydroxyisoquinoline-1,3(2*H*,4*H*)-dione scaffold consists of the condensation of homophthalic acid derivatives with *O*-benzylhydroxylamine to obtain the corresponding 2-benzyloxyisoquinoline-1,3(2*H*,4*H*)-diones followed by deprotection of the *N*-hydroxy function (Scheme 1).[33] We adapted this scheme to elaborate three series of 7-substituted-2-hydroxyisoquinoline-1,3(2*H*,4*H*)-diones. The first series was dedicated to small groups such as nitro, amino, halide, and hydroxyl groups [**6b**−**g** (Table 1)]. The second and third ones incorporated various amide groups [**6h**−**n** (Table 1)] and substituted aryl groups [**6o**−**s** (Table 1)], respectively.

Table 1. Inhibition of HIV-1 IN and RT RNase H Activities, Antiviral Activity, and Cytotoxicity of 7-Substituted 2-Hydroxyisoquinoline-1,3(2*H*,4*H*)-dione Compounds.

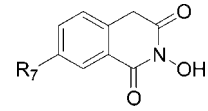

		IC_{50} (μM)				
compd	R_7	overall IN[a]	RT RNase H[b]	RNase H/IN[c]	EC_{50}[d] (μM)	CC_{50}[e] (μM)
6a	H	6.32 ± 2.61	5.9 ± 1.4	0.9	NT[f]	NT[f]
6b	NO_2	8.50 ± 3.24	48.0 ± 0.7	5.6	>205	>205
6d	Cl	0.80 ± 0.09	28.9 ± 6.0	36.1	>48	>48
6e	Br	0.58 ± 0.50	>96.00 ± 7.1	165.5	>64	>64
6f	I	1.22 ± 0.03	58.0 ± 0.7	48.3	>70	>70
6g	OH	2.22 ± 0.20	37.4 ± 2.5	17.0	>48	>48
6h	$NHCOCH_3$	0.59 ± 0.32	40.7 ± 15.5	69.0	148	>250
6i	$NHCOC_4H_9$	18.80 ± 15.77	>80.0	4.2	>250	>250
6j	NHCOPh	1.24 ± 1.04	5.7 ± 1.5	4.7	22	84
6k	NHCO(4-F)Ph	0.41 ± 0.00	7.1 ± 5.4	17.3	>120	>120
6l	NHCO(3-NO_2)Ph	8.90 ± 3.11	10.8 ± 2.1	1.2	NT[f]	NT[f]
6m	$NHCOCH_2Ph$	0.09 ± 0.08	>80.0	888.9	>121	>121
6n	$NHCOCH_2$(4-F)Ph	0.13 ± 0.00	35.3 ± 2.9	271.5	>116	>116
6o	4-F-Ph	1.47 ± 0.47	22.2 ± 10.6	15.8	>46	>46
6p	4-CF_3-Ph	1.80 ± 1.12	10.7 ± 2.8	5.9	>47	>47
6q	Ph	1.73 ± 1.18	>80.0	47.0	>66	>66
6r	4-OH-Ph	5.42 ± 0.14	7.2 ± 1.1	1.3	>186	>186
6s	3,4-diOH-Ph	0.56 ± 0.34	6.6 ± 0.5	11.8	>89	>89

[a] Concentration required to inhibit by 50% the in vitro overall integrase activity. Values are means ± standard deviations from at least three independent experiments. [b] Concentration required to inhibit by 50% the in vitro RNase H activity. [c] $IC_{50\ RNase\ H}/IC_{50\ HIV\text{-}1\ IN}$ ratio. [d] Effective concentration required to reduce the HIV-1-induced cytopathic effect by 50% in MT-4 cells. [e] Cytotoxic concentration required to reduce MT-4 cell viability by 50%. [f] Not tested.

The main precursor of **6b**−**g** was 5-nitrohomophthalic acid **2** (Scheme 2), which was obtained by a selective nitration of homophthalic acid **1**.[34,35] Reduction by catalytic hydrogenation on 5% Pd/C afforded 5-aminohomophthalic acid **3** in very good yield. Diazotation by sodium nitrite in acid medium gave the diazonium salt, which was allowed on the one hand to react with cuprous halides to afford the 5-chloro-, 5-bromo-, and 5-iodohomophthalic acids **4a**−**c**. On the other hand, hydrolysis by hot sulfuric acid gave 5-hydroxyhomophthalic acid **4d**.

All these 7-substituted homophthalic acids as well as commercial homophthalic acid **1** were cyclized with *O*-benzylhydroxylamine in toluene at reflux in a Dean−Stark apparatus to give the 2-benzyloxyisoquinoline-1,3(2*H*,4*H*)-dione derivatives **5a**−**g**. The corresponding deprotected 2-hydroxyisoquinoline-1,3(2*H*,4*H*)-diones **6a**−**g** were obtained via the action of boron tribromide at room temperature (Scheme 1 and Table 1). BBr_3 deprotection was preferred to the previously reported catalytic hydrogenation since reaction was faster (1 h) and reduction of the nitro group was avoided (**6b**).

Substitution at position 7 with amido groups (second series) was accomplished using two methods. In the first method,

Scheme 2. Synthesis of 7-Substituted Homophthalic Acid Precursors[a]

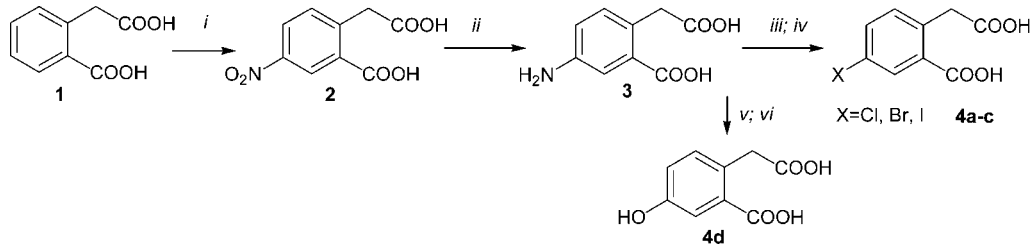

[a] Reagents and conditions: (i) fuming HNO_3, 0 °C, 2 h; (ii) H_2, 5% Pd/C, MeOH; (iii) $NaNO_2$, HX, 5 °C; (iv) CuX, HX, 5 °C, 2 h; (v) $NaNO_2$, H_2SO_4, 5 °C; (vi) H_2SO_4, H_2O, reflux.

Scheme 3. Synthesis of Homophthalic Anhydrides **7a−c** and Homophthalic Acids **7d−g**[a]

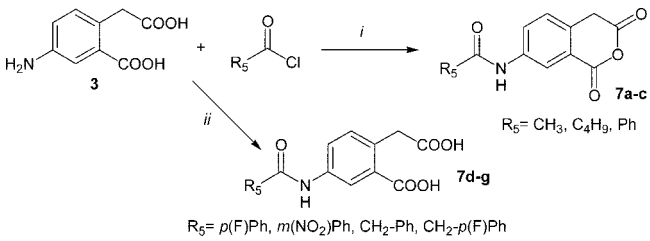

[a] Reagents and conditions: (i) 8.0 equiv of R_5COCl, 90 min, reflux; (ii) (a) 1.0 equiv of R_5COCl, 2.0 N KOH, 2 h, room temperature, (b) 2.0 N HCl, room temperature.

5-aminohomophthalic acid **3** was refluxed in 8 equiv of the desired acyl chloride to yield the homophthalic anhydrides **7a−c** (Scheme 3). In the second method, 5-aminohomophthalic acid **3** was treated with the acyl chloride in a 2.0 N KOH solution at room temperature to yield the homophthalic acids **7d−g** after acidification (Scheme 3).

As described in Scheme 1, **7a−g** were cyclized giving the 2-benzyloxy compounds **5h−n** and deprotected by treatment with boron tribromide affording **6h−n** (Table 1). It was possible to elaborate **6h** in one step from **7a** by refluxing with hydroxylamine.

The third series was built up on a Suzuki coupling reaction between commercially available boronic acids and either a 5-halogenohomophthalic acid or a 2-benzyloxy-7-halogenoisoquinoline-1,3(2*H*,4*H*)-dione. Scheme 4 shows the two best investigated synthetic schemes for the obtention of the precursor of **6q** (i.e., **5q**) since preliminary experiments evidenced that some routes were unsuccessful. Route A, in which 2-benzyloxy-5-bromoisoquinoline-1,3(2*H*,4*H*)-dione **5e** was allowed to react with phenylboronic acid, gave **5q** in 38% overall yield. Route B, in which 5-iodohomophthalic acid **4c** was coupled with phenylboronic acid, giving 5-phenylhomophthalic acid **7h** followed by cyclization with *O*-benzylhydroxylamine, afforded **5q** in 42% yield. In route A, the Suzuki coupling reaction of phenyl boronic acid with 2-benzyloxy-7-chloroisoquinoline-1,3(2*H*,4*H*)-dione **5d** led quantitatively to starting material recovery, whereas the use of the analogous iodinated compound **5f** led mainly to 5-phenylhomophthalic acid **7h** (98%) with only traces of desired compound **5q**. In the last case, the degradative opening of the isoquinoline ring was attributed to the presence of the catalyst $Pd(P\Phi_3)_4$ since the same phenomenon was observed when **5f** afforded 5-iodohomophthalic acid **4c** (80% yield) after treatment with the catalyst in the absence of phenylboronic acid. In route B, the Suzuki coupling reaction of 5-bromo- and 5-chlorohomophthalic acid (**4a** and **4b**, respectively) with phenylboronic acid did not occur. Routes A and B were used for the synthesis of **5o−q** and **5q−s**, respectively, and a final deprotection via the action of boron tribromide afforded the 7-aryl-2-hydroxyisoquinoline-1,3(2*H*,4*H*)-diones **6o−s** (Table 1).

Finally, the whole series of 2-hydroxyisoquinoline-1,3(2*H*,4*H*)-diones comprises 19 compounds obtained as mixtures of keto and enol forms with a large preference for the keto form (Scheme 1 and Table 1). The protected precursors also gave mixtures of keto and enol forms. We also synthesized **6t**, i.e., 3-hydroxy-2*H*-1,3-benzoxazine-2,4(3*H*)-dione according to a previously reported method.[36] This is an analogue of **6a** in which the methylene group at position 4 is replaced with an oxygen atom.

Biology. Table 1 reports the enzyme inhibitory activities as well as the antiviral properties of this series of 2-hydroxyisoquinoline-1,3(2*H*,4*H*)-diones. It is noteworthy that **6c** (R_7 = NH_2) could not be tested due to solubility problems. Klumpp et al. reported that *N*-hydroxyimide **6a** inhibited HIV RNase H activity with an IC_{50} value of ~1.0 μM.[31] We obtained an IC_{50} value of 5.9 μM. Typical inhibition curves are shown in Figure 1. The discrepancy between these two results may be attributed to the different conditions of the enzyme activity assays. Klumpp et al.[31] used G20 RNA hybridized to D1 DNA double-stranded DNA−RNA hybrid substrate, whereas we use ^{3}H-labeled RNA transcribed from single-stranded calf thymus by *Escherichia coli* RNA polymerase. Substitution at position 7 with various groups does not lead to any major improvement in the RNase H inhibitory activity (Table 1). **6j** has a similar IC_{50} value (5.7 μM), whereas **6k**, **6l**, **6p**, **6r**, and **6s** are slightly less inhibitory (6.6−10.8 μM). Introduction of an arylcarbonylamino group (**6j−l**) or of a hydroxylated phenyl ring (**6r,s**) at position 7 retains the inhibitory activity of lead compound **6a**. On the other hand, introduction of a nitro (**6b**), a halide (**6d−f**), a hydroxyl (**6g**), an alkylcarbonylamino (**6h,i**), or an alkarylcarbonylamino (**6m,n**) group is not favorable for inhibition. One should notice the great influence of the substituent on the phenyl ring in position 7 on the inhibitory activity. **6q** is not active at concentrations of up to 60.0 μM, whereas its substituted counterparts (**6o,p** and **6r,s**) exhibit various IC_{50} values from 6.6 to 22.2 μM.

In contrast to the RNase H results, the HIV-1 IN inhibitory activities (Table 1) are noticeable and strongly influenced by the nature of the substituent at position 7. All compounds inhibit overall HIV-1 IN activity with IC_{50} values ranging from 0.09 to 18.8 μM, and seven compounds (**6d**, **6e**, **6h**, **6k**, **6m**, **6n**, and **6s**) show submicromolar IC_{50} values. **6m** and **6n** are the best ones of the series with IC_{50} values of ~0.1 μM. A group of six molecules (**6f**, **6g**, **6j**, and **6o−q**) displays IC_{50} values between 1.0 and 2.0 μM. Except for three compounds, **6b**, **6i**, and **6l**, all the 7-substituted 2-hydroxyisoquinoline-1,3(2*H*,4*H*)-diones are more active than reference compound **6a** (6.3 μM). The discovery of **6m** and **6n** as new hits in the field of HIV-1

Scheme 4. Best Routes for the Synthesis of 2-Benzyloxy-7-phenylisoquinoline-1,3(2*H*,4*H*)-dione **5q**[a]

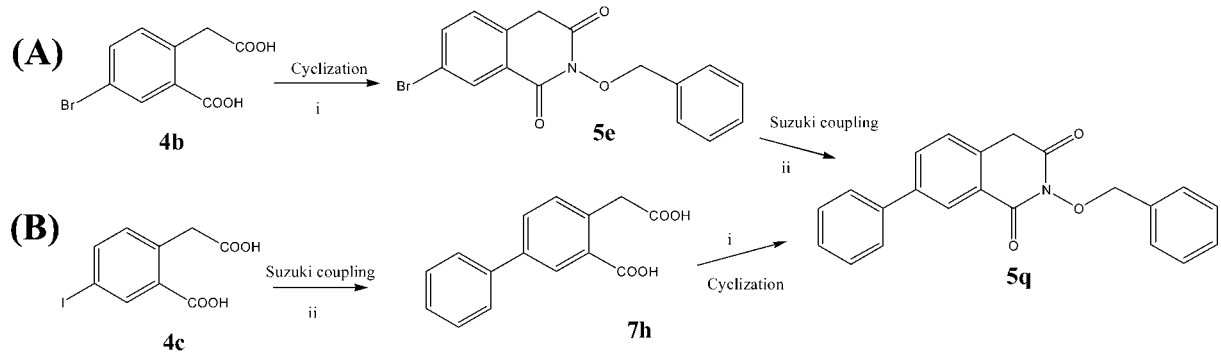

[a] Reagents and conditions: (i) 1.2 equiv of NH_2OBn, toluene, Dean−Stark apparatus, reflux, 12 h; (ii) 1.0 equiv of $\Phi B(OH)_2$, $Pd(P\Phi_3)_4$, 2.0 M K_2CO_3, benzene, reflux, 3 h.

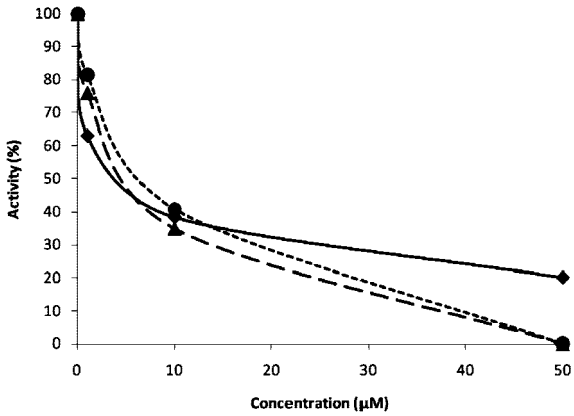

Figure 1. Typical RNase H inhibition curves for (◆) **6a**, (●) **6k**, and (▲) **6r**.

Table 2. Inhibition of HIV-1 IN Catalytic Activities of **6e**, **6m**, **6n**, and Some Reference Compounds

	IC_{50} (μM)			
compd	3′-P[a]	ST[b]	overall[c]	3′-P/ST[d]
6e	1.40 ± 0.04	0.90 ± 0.08	0.58 ± 0.35	1.6
6m	7.79 ± 4.25	0.10 ± 0.05	0.09 ± 0.00	77.9
6n	0.75 ± 0.40	0.02 ± 0.01	0.13 ± 0.00	37.5
Raltegravir	0.90 ± 0.42	0.0070 ± 0.0005	0.009 ± 0.0002	128.6
Elvitegravir	0.05 ± 0.01	0.0070 ± 0.0007	0.004 ± 0.003	7.1
L-870,810	0.12 ± 0.03	0.0025 ± 0.0007	0.0005 ± 0.0003	48.0

[a] Concentration required to inhibit by 50% the in vitro 3′-processing integrase activity. [b] Concentration required to inhibit by 50% the in vitro strand transfer integrase activity. [c] Concentration required to inhibit by 50% the in vitro overall integrase activity. [d] IC_{50} 3′-P/IC_{50} ST ratio.

IN inhibitors prompted us to investigate their pharmacological properties. Table 2 shows the inhibition of the HIV-1 IN 3′-processing (3′-P), strand transfer (ST), and overall integrase activities by **6m**, **6n**, and **6e** (the third best candidate of the series) together with known reference compounds. Except for **6e** that displays similar IC_{50} values for 3′-P and ST, the inhibition of integrase activity at submicromolar concentrations of **6m** and **6n** was due to inhibition of ST in a low submicromolar range. **6m**, **6n**, and the diketo acid-like compound L-870,810 displayed similar IC_{50} 3′-P/IC_{50} ST ratios. Nevertheless, the overall IC_{50} values of **6m** and **6n** remain modest in comparison to those of the reference compounds. They are 10-, 50-, and 200-fold less active than Raltegravir, Elvitegravir, and L-870,810, respectively.

Figure 2 shows a reciprocal plot of IC_{50} values for integrase and RNase H. All the compounds are located in the upper part of the graphics showing their modest properties as RNase H

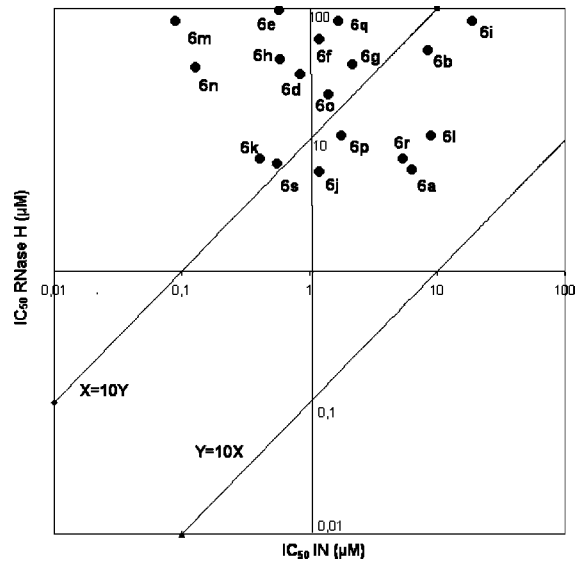

Figure 2. Correlation between HIV-1 integrase and RNase H inhibition.

inhibitors. **6m** and **6n** with high $IC_{50\ RNase\ H}/IC_{50\ HIV\text{-}1\ IN}$ ratios of 889 and 271, respectively (Table 1), are the compounds which are the most selective for HIV-1 IN since they are highly potent HIV-1 IN inhibitors and, on the other hand, inactive as RNase H inhibitors. Then a group composed of **6d**, **6e**, **6f**, **6h**, and **6q** offers an approximately 5−25-fold decrease in selectivity for HIV-1 IN when compared to the best candidate **6m** (ratios between 36 and 165). IC_{50} ratios are lower for these compounds with less favorable HIV-1 IN inhibitory properties. Finally, **6g**, **6k**, **6o**, and **6s** near the straight line $X = 10Y$ (Figure 2) display very modest selectivity for HIV-1 IN, whereas the remaining compounds clustered around the center of the graph (**6a**, **6j**, **6l**, **6p**, and **6r**) are dual inhibitors.

Most of the compounds were tested as RT RNA-dependent DNA polymerase inhibitors. For most of the compounds, a maximum inhibition of 40% was attained at 50 μM (Figure 3). Compounds **6o**, **6r**, and **6s** exhibited 60, 50, and 70% inhibition, respectively, at 50 μM. A slight stimulation of RT should be noticed for low inhibitor concentrations. It is also noteworthy that the benzoxazine analogue **6t** did not display any activity in the enzymatic assays.

Finally, the antiviral properties were investigated by MT-4/MTT assays. All the compounds displayed important cytotoxicity, which hindered the detection of any antiviral activity in cell culture (Table 1). Only **6j** was found to display a modest antiviral activity with a therapeutic index of ∼4.

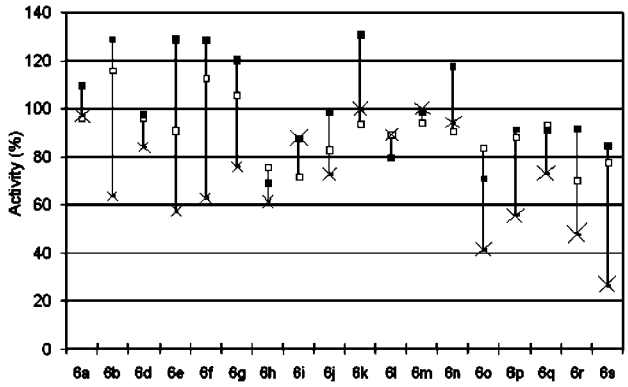

Figure 3. Effect of compounds on DNA polymerase activity. The DNA polymerase activity of RT was assayed in the presence of increasing concentrations of compounds. RT was preincubated for 10 min at 37 °C with the inhibitors, and then incubation was carried out for an additional 10 min. Reaction was stopped with trichloroacetic acid, and radioactivity was measured as described in the Experimental Section: (□) 1.0, (■) 10.0, and (×) 50.0 μM.

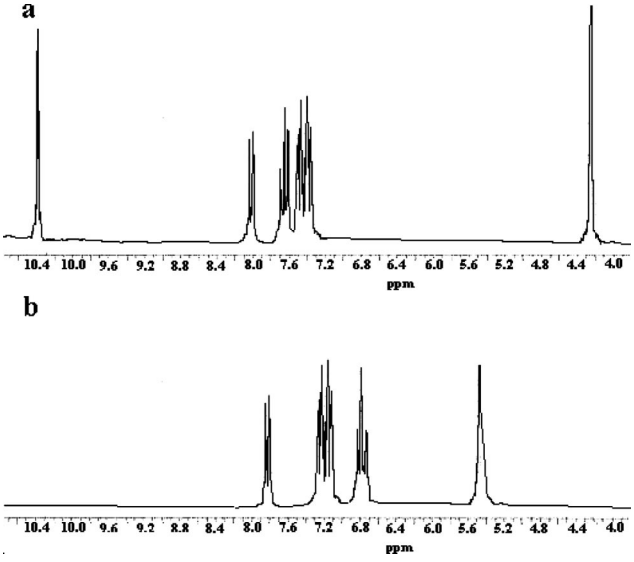

Figure 4. ^{1}H NMR spectra of (a) a 0.01 M solution of **6a** in DMSO-d_6 and (b) a 0.01 M solution of **6a** with 1.0 equiv of $Mg(OAc)_2 \cdot 4H_2O$.

Physicochemical Studies. The biological data highlight the large selectivity of **6m** and **6n** for HIV-1 IN. Since the strong HIV-1 IN inhibitory potencies of the β-diketo acids (DKAs) are mostly attributed to their metal ion chelating abilities, we decided to investigate the magnesium-chelating capacities for reference compound **6a** and the most active one, **6n**. First, ^{1}H NMR studies gave useful information about the interaction of **6a** with magnesium ion. Figure 4a shows the ^{1}H NMR spectrum of a 0.01 M solution of **6a** in DMSO-d_6. Upon addition of $Mg(OAc)_2 \cdot 4H_2O$ (1 equiv), this spectrum was strongly modified (Figure 4b). The singlet at 4.26 ppm characteristic of the methylene (2H, H_4) was replaced by a broad singlet at 5.55 ppm (1H, H_4) characteristic of an enolic proton. The singlet at 10.4 ppm (1H, OH) disappeared, and the signals for the aromatic protons were variously shifted toward the high fields (Table 3). Since water is present in the magnesium acetate complex, we verified that there was no interference of water in the ^{1}H NMR spectrum of **6a**. Its spectrum in the presence of 6% water was not modified. This first study indicated that the acetate anion could be responsible for the enolization of the carbonyl function in position 3 into enolate, and then we studied the effect of

Table 3. Changes in ^{1}H Chemical Shifts ($\Delta\delta$) for the Complexation of **6a** with Various Salts

complex[a]	$\Delta\delta$ (H_4)	$\Delta\delta$ (H_5)	$\Delta\delta$ (H_6)	$\Delta\delta$ (H_7)	$\Delta\delta$ (H_8)
6a with 1.0 equiv of $Mg(OAc)_2 \cdot 4H_2O$	+1.24	−0.35	−0.87	−0.35	−0.23
6a with 1.0 equiv of $MgCl_2$	+3.24	+0.40	+0.40	+0.40	+0.16
6a with 2.0 equiv of NaOAc	+0.89	+0.35	−0.60	−0.90	−1.10
6a with 2.0 equiv of NaOH	+0.89	+0.35	−0.60	−0.90	−1.10

[a] NMR experiments were conducted in 0.01 M solutions of **6a** in DMSO-d_6 at room temperature.

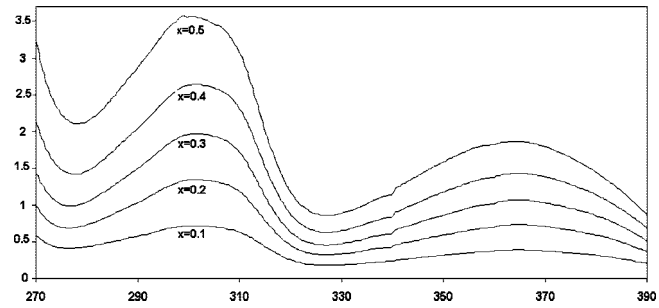

Figure 5. Absorption spectra of **6a** (x milliliters of a 10^{-3} M methanolic solution) in the presence of $Mg(OAc)_2 \cdot 4H_2O$ ($1 - x$ mL of a 10^{-3} M methanolic solution). The same amount of **6a** was put into the reference cuvette.

$MgCl_2$. In the presence of 1.0 equiv of $MgCl_2$ and after incubation for 7 days, a new species appeared. Its concentration increased with time (14 days), but there was still an important proportion of the original form. The NMR data for this new species (Table 3) attested to the very slow formation of the enolic form. So the quantitative formation of the enolic form requires the presence of proximal basic anions, and to investigate the effect of this anion, we recorded the spectra of **6a** in the presence of 2.0 equiv of NaOAc [to be under the same pH conditions as with $Mg(OAc)_2$]. The global evolutions of the ^{1}H NMR spectrum were similar to those observed in the presence of $Mg(OAc)_2$. The singlets characteristic of the methylene (H_4) and hydroxy protons rapidly disappeared, and there were highfield shifts (Table 3) for the aromatic proton signals (H_6, H_7, H_8). However, these shifts were greater with NaOAc than with $Mg(OAc)_2$, indicating clearly the intervention of the magnesium cation in the complex formation. A similar study with 2.0 equiv of NaOH led to the same spectrum recorded with NaOAc. In the presence of the strongly basic hydroxide anion, the bianionic form of **6a** (deprotonation of the hydroxy function and formation of the enolate) was undoubtedly obtained, and it appears that the less basic acetate anion could play the same role as previously described for β-diketo acid metal complexes.[37]

Second, UV−vis experiments allowed us to confirm the stoichiometry of the magnesium complexes. We used a Job plot experiment. The UV−vis spectrum of **6a** was sharply affected by the addition of the magnesium cation with large hyperchromic effects at 302 and 365 nm. Figure 5 shows the UV−vis spectra obtained according to the continuous variation method for increasing ligand volumic fractions x. The maximum effect was obtained for $x = 0.5$, and an isobestic point was observed at 281 nm. For greater values of x, there was a decrease in absorbance accounting for a decrease in the complex concentration due to the lack of magnesium cations. This accounts for a 1/1 stoichiometry, which was ascertained by the Job plot (Figure 6). The association constant K of the complex evaluated from the absorption data was found to be 3.0×10^4 M^{-1}. Similar

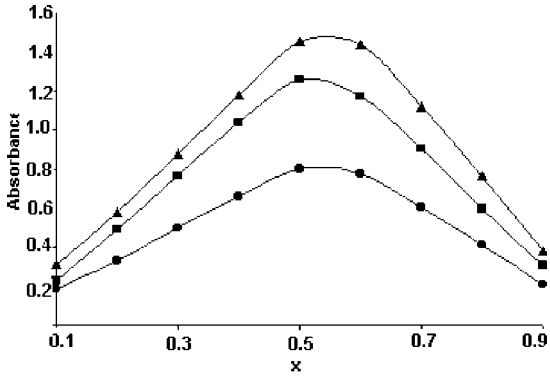

Figure 6. Job plots of **6a** with Mg^{2+}: (●) 5×10^{-4} M and $\lambda = 365.5$ nm, (■) 5×10^{-4} M and $\lambda = 302.5$ nm, and (▲) 8×10^{-4} M and $\lambda = 365.5$ nm.

UV−vis experiments were performed with **6m** and evidenced the same 1/1 stoichiometry with an association constant of 5.9×10^3 M^{-1}.

As far as the benzoxazine analogue **6t** is concerned, the ^1H NMR spectrum was only very slightly modified upon addition of sodium acetate and magnesium acetate. The singlet corresponding to the hydroxy function disappeared, accounting for its deprotonation by the basic acetate anion, and UV−vis titration also revealed slight modifications of the spectrum. The magnesium complexation may occur only slowly, and a very low association constant may hinder the evidence of complex formation.

Three-Dimensional (3D) QSAR Analysis. The submicromolar HIV-1 IN inhibitory properties of **6m** and **6n** led us also to investigate their putative fits into the HIV-1 IN active site. For that purpose we used a previously reported 3D quantitative pharmacophore model for diketo acids.[38] The selected 3D hypothesis consisted of four features in a specific three-dimensional orientation: two hydrogen bond acceptors (HBA1 and HBA2), one hydrogen bond donor (HBD), and one hydrophobic aromatic region (HYAr). The superimposition of lead compound **6a** onto this pharmacophore model showed that **6a** mapped to only three of the four features with a predicted IC_{50} value of 57 μM (Figure 7A). The introduction of the phenylacetamido group in position 7 allowed **6m** to interact with the fourth feature of the hypothesis (HYAr), and its predicted IC_{50} was 0.64 μM (Figure 7B). The results obtained by the use of this 3D pharmacophore model are in accordance with the experimental biological data.

Discussion

2-Hydroxyisoquinoline-1,3(2*H*,4*H*)-dione **6a** or *N*-hydroxyimide was previously designed and discovered as a lead compound, consistent with a pharmacophore model for the binding to the two-metal ion active site of influenza endonuclease. In this pharmacophore, the catalytic divalent metal ions are bound at a distance of 4−5 Å in the active site, and each metal ion interacts with two of three compound oxygen atoms at a distance of 2−2.5 Å.[32] Subsequent tests revealed *N*-hydroxyimide as a potent inhibitor of HIV RNase H activity, confirming the two-metal ion mechanism of RNA cleavage.[31] Herein, we developed a series of 7-substituted analogues and tested them against three catalytic HIV-1 enzyme activities: RT polymerase, RT RNase H, and integrase. Most compounds exhibited only weak antipolymerase activity, except compound **6s** with 70% inhibition at 50 μM. Most compounds were selective for HIV-1 IN with an IC_{50} in the micromolar range,

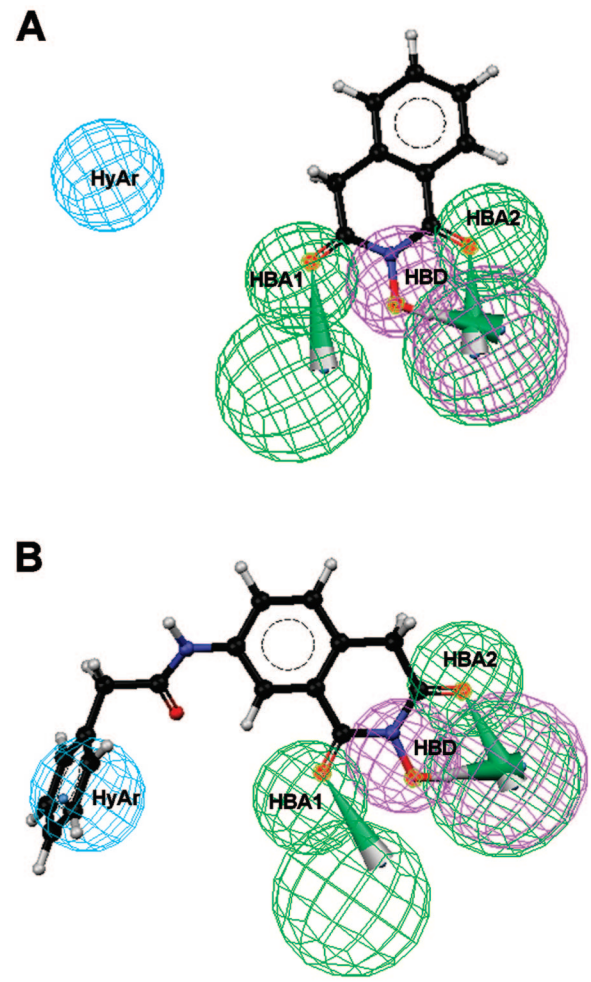

Figure 7. HypoGen pharmacophore model aligned with **6a** (A) and **6m** (B).

and two compounds, **6m** and **6n**, active in the submicromolar range displayed a high selectivity for HIV-1 IN. The structural requirement for this HIV-1 IN specificity seems to be the presence of a phenylacetamido group in position 7, which allows for a good fit onto a 3D pharmacophore model for diketo acids. Fitting the hydrophobic aromatic region also induced a high selectivity for strand transfer, to which the low 3′-P/ST ratio of **6e** compared to the high ratios of **6m** and **6n** attests (Table 2). This is the first anti-integrase activity reported for *N*-hydroxyimides that were so far only studied as potential RNase H inhibitors. When compared to those of lead compound **6a**, the RNase H inhibitory properties of several analogues were similar, and no clear structure−activity relationship emerged from the IC_{50} values. The pharmacomodulation of the isoquinoline ring in position 7 did not yield better candidates than **6a**, and we did not obtain compounds active in the submicromolar range against RNase H in contrast to some of the madurahydroxylactone derivatives reported by Marchand et al.[29] The compounds with the best anti-RNase H activities were located around the center of the reciprocal plot of IC_{50} values (Figure 2), revealing a modest dual inhibition of both enzymes. This situation is comparable to the one encountered for previously reported hydroxytropolones,[26] which in addition inhibited RT polymerase in most cases. In contrast, *N*-hydroxyimides, like a thiophenyl diketo acid,[23] did not inhibit RT polymerase. However, one should notice that the absence of homogeneity under the published RNase H assay conditions renders the strict comparison between the different IC_{50} values very difficult.

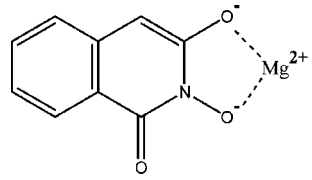

Figure 8. Structure of the complex of **6a** with Mg^{2+}.

For the first time, we also investigated the magnesium chelating properties of this series of compounds in detail. The physicochemical data obtained from NMR and UV−vis experiments were in full accordance and consistent with a 1/1 stoichiometry for the magnesium complex (Figure 8). The magnesium ion is coordinated to the isoquinoline ring via the hydroxy function in position 2 and the enolate in position 3. This enol form, which was minor (0−30%) in ligand NMR spectra, was characterized in the magnesium complex. Thus, the keto−enol equilibrium shifted significantly in favor of the enol tautomer upon metal binding, and this shift was critical for the interaction with metal ions since the benzoxazine analogue **6t** lacking the enolization ability did not bind the magnesium cation. Furthermore, this benzoxazine analogue was also devoid of any enzymatic inhibitory activity, suggesting that the anti-IN and anti-RNase H activities of 2-hydroxyisoquinoline-1,3(2*H*,4*H*)-diones can be related to their metal binding capacities. The physicochemical experiments are in favor of a 1/1 metal−ligand complex. In contrast, *N*-hydroxyimide **6a** was discovered by screening of a targeted subset of the Roche compound library as an inhibitor of influenza endonuclease, which may bind simultaneously two metal ions of the enzymatic catalytic site.[32] This metal binding ability was presumed for **6a** on the basis of structural comparisons with other well-known metal-chelating compounds. No detailed study on this magnesium complex (structure, stoichiometry, etc.) has been published. A NMR spectral change consistent with enol formation occurred upon interaction of **6a** with Mg^{2+} or with the isolated HIV RNase H domain in the presence of Mg^{2+}.[32] An analogue was also shown to bind specifically to the isolated HIV RNase H domain by protein fluorescence quenching with a stoichiometry of one ligand molecule per protein molecule.[30] No clear ligand/metal stoichiometry emerged from these studies. The intrinsic selectivity of **6a** for two metal ion active sites is significant because no inhibition of *E. coli* RNase HI (one-metal ion active site) was detected at concentrations that led to almost complete inhibition of HIV RNase H (two-metal ion active site).[30] However, one cannot firmly form conclusions about the ligand/metal stoichiometry for two major reasons: there is no published crystal structure of a protein−ligand complex, and the number of metal ions in the catalytic RNase H active sites is still subject to debate. Here we show a 1/1 stoichiometry in the absence of protein. This may reflect the best strong metal chelating site of the ligand in solution, but it may also interact with a second metal ion by a perfect fit into a catalytic active site.

The common structural features of the catalytic centers for HIV-1 IN, RT RNase H, and RT polymerase highlight the interest in these enzymes as pharmacological targets for the design of novel anti-HIV compounds. With the growing emergence of drug resistance, it is important to develop novel highly specific enzymatic inhibitors as it is the case for most of the commonly used anti-HIV drugs. HIV-1 RT RNase H is an insufficiently exploited target. The search for dual or trial enzymatic inhibitors may be fruitful as well. The antiviral activity of these compounds in cell culture could not be demonstrated as a result of cytotoxicity. This toxicity could be explained by an effect of the compounds on other cellular bimetallic enzymes, and one could argue that it will be impossible to find compounds that will be specific for HIV-1 enzymes without revealing deleterious toxicities. In this respect, DKAs and their derivatives represent one of the major leads in the development of anti-HIV-1 IN drugs.[39] They were found to selectively inhibit the strand transfer step by sequestering the divalent cations bound in the active site of the enzyme[40] and to block HIV-1 replication in infected cells. In spite of their metal binding capacities, they exhibited low toxicities, and the derived bioisosteres could enter into clinical trials. S-1360 was the first one, for which clinical investigation was stopped due to its metabolic instability but not to its cytotoxicity.[41,42] Currently, GS-9137 is in advanced stages of clinical trials,[10] and the first U.S. FDA-approved anti-IN drug as of October 2007, Raltegravir, exhibited excellent therapeutic efficacy in antiretroviral treatment-naive and treatment-experienced HIV-1-infected patients.[11,12] Consistent with the specificity of these three major compounds to IN, IN mutant proteins have been isolated.[43,44] The recent design of dual inhibitors of HIV-1 IN and RT combining a diketo acid moiety with a non-nucleoside RT inhibitor also illustrates that it is possible to obtain compounds inhibiting HIV-1 RT and IN with remarkably high therapeutic indexes in cell-based assays.[45] Within the same scaffold, cytotoxicity may be largely influenced by the modulation of a single substituent, as exemplified by the studies of Sato et al. on a series of HIV-1 IN-targeted quinolone derivatives.[46] These different examples show that inhibitors interfering with metal ions in the enzyme catalytic sites can be specific and weakly cytotoxic. Therefore, 2-hydroxyisoquinoline-1,3(2*H*,4*H*)-dione is a scaffold that must be further structurally investigated. We are currently studying novel series of compounds variously substituted at other positions of the heterocycle. Perhaps some compounds will reveal a high specificity for RNase H. Using the structures of the last generation of IN inhibitors (Elvitegravir and Raltegravir), a new multipoint pharmacophore model including a previously unexplored region has been refined.[47] When we start from the structures of **6m** and **6n**, fitting this region by additional convenient substituents may allow us to improve the antiviral and cytotoxic properties of this family and to gain further insights into the structural requirements for enzyme selectivity. These studies will be reported in due course.

Experimental Section

Chemistry. General Details. All reagents and solvents were purchased from Aldrich-Chimie (Saint-Quentin-Fallavier, France), were ACS reagent grade, and were used as provided. Thin layer chromatography analyses were performed on plastic sheets precoated with silica gel 60F254 (Merck). SiO_2, 200/400 mesh (Merck), was used for column chromatography. NMR spectra were obtained on an AC 300 Bruker spectrometer in the appropriate solvent with TMS as an internal reference. Chemical shifts are reported in δ units (parts per million) and are assigned as singlets (s), doublets (d), doublets of doublets (dd), triplets (t), quartets (q), quintets (quin), sextuplets (sext), multiplets (m), and broad signals (br). Melting points were obtained on a Reichert Thermopan melting point apparatus, equipped with a microscope, and are uncorrected. Mass spectra were recorded on a Thermo-Finnigan PolarisQ mass spectrometer (70 eV, Electronic Impact). Elemental analyses were performed by CNRS laboratories (Vernaison).

Synthesis of Homophthalic Acid Derivatives. (i) 2-Carboxymethyl-5-nitrobenzoic Acid (2). Fuming nitric acid (20 mL) was cooled to 0 °C, and 6.25 g of homophthalic acid (35.0 mmol) was carefully added while the temperature was kept below 22 °C. After 2 h, ice (20 g) was added. The precipitate was filtered and washed

several times with distilled water. After the sample was dried at room temperature, **2** was obtained as a white powder: 90% yield; mp 235 °C; ^{1}H NMR (DMSO-d_6) δ 4.06 (s, 2H, CH_2), 7.66 (d, 1H, ^3J = 8.5 Hz, H_3), 8.34 (dd, 1H, ^3J = 8.5 Hz, ^4J = 2.4 Hz, H_4), 8.61 (d, 1H, ^4J = 2.4 Hz, H_6); ^{13}C NMR (DMSO-d_6) δ 39.3 (CH_2), 123.6 (CH), 125.5 (CH), 128.6 (CH), 131.0 (C_1), 139.6 (C_2), 150.2 (C_5), 164.3 (CO), 174.0 (CO).

(ii) 5-Amino-2-carboxymethylbenzoic Acid (3). 2-Carboxymethyl-5-nitrobenzoic acid **2** (2.25 g, 10.0 mmol) was solubilized in methanol (10 mL) and hydrogenated on 0.2 g of 5% Pd/C under normal pressure. Water (50 mL) was added, and the mixture was refluxed for 5 min. After filtration of the hot solution, **3** slightly crystallized at room temperature as orange needles, which were washed with cold water and dried at room temperature: 80% yield; mp 218 °C; ^{1}H NMR (DMSO-d_6) δ 3.70 (s, 2H, CH_2), 6.66 (dd, 1H, ^3J = 8.2 Hz, ^4J = 2.4 Hz, H_4), 6.92 (d, 1H, ^3J = 8.2 Hz, H_3), 7.15 (d, 1H, ^4J = 2.4 Hz, H_6); ^{13}C NMR (DMSO-d_6) δ 39.5 (CH_2), 115.1 (CH), 117.2 (CH), 123.5 (C_2), 128.5 (CH), 131.0 (C_1), 148.4 (C_5), 161.3 (CO), 173.8 (CO).

(iii) 5-Halogeno-2-carboxymethylbenzoic Acids (4a−c). 5-Amino-2-carboxymethylbenzoic acid **3** (1.00 g, 5.1 mmol) was dissolved at 5 °C in a concentrated HX acid solution (3.0 mL of HCl, HBr, or HI). A solution of sodium nitrite (0.534 g, 5.1 mmol) in water (3.0 mL) was slowly added while the temperature was kept below 5 °C to yield a pink solution of the diazonium salt. A cold solution of CuX (5.1 mmol) in a concentrated HX acid solution was added dropwise to the diazonium mixture while the temperature was kept below 5 °C. After the mixture had been stirred for 2 h and the temperature had risen, 5-halogeno-2-carboxymethylbenzoic acids precipitated at room temperature. Solids were filtered, washed with distilled water, and dried at room temperature.

(iv) 2-Carboxymethyl-5-chlorobenzoic acid (4a): brown solid; 72% yield; mp 203 °C; ^{1}H NMR (DMSO-d_6) δ 3.92 (s, 2H, CH_2), 7.36 (d, 1H, ^3J = 8.2 Hz, H_3), 7.59 (dd, 1H, ^3J = 8.2 Hz, ^4J = 2.1 Hz, H_4), 7.84 (d, 1H, ^4J = 2.1 Hz, H_6); ^{13}C NMR (DMSO-d_6) δ 39.5 (CH_2), 128.9 (CH), 129.1 (CH), 130.9 (CH), 131.5 (C), 131.6 (C), 136.5 (C_5), 160.3 (CO), 173.6 (CO).

(v) 5-Bromo-2-carboxymethylbenzoic acid (4b): salmon solid; 93% yield; mp 215 °C; ^{1}H NMR (DMSO-d_6) δ 3.91 (s, 2H, CH_2), 7.31 (d, 1H, ^3J = 8.0 Hz, H_3), 7.72 (dd, 1H, ^3J = 8.0 Hz, ^4J = 2.0 Hz, H_4), 7.98 (d, 1H, ^4J = 2.0 Hz, H_6); ^{13}C NMR (DMSO-d_6) δ 39.5 (CH_2), 124.2 (C_5), 129.3 (CH), 131.6 (CH), 131.8 (C), 131.9 (C), 133.6 (CH), 159.8 (CO), 174.0 (CO).

(vi) 2-Carboxymethyl-5-iodobenzoic acid (4c): orange solid; 73% yield; mp 280 °C; ^{1}H NMR (DMSO-d_6) δ 3.88 (s, 2H, CH_2), 7.12 (d, 1H, ^3J = 8.0 Hz, H_3), 7.85 (dd, 1H, ^3J = 8.0 Hz, ^4J = 1.8 Hz, H_4), 8.16 (d, 1H, ^4J = 1.8 Hz, H_6); ^{13}C NMR (DMSO-d_6) δ 39.5 (CH_2), 93.1 (C_5), 129.3 (CH), 131.8 (C_1), 134.6 (C_2), 137.4 (CH), 139.3 (CH), 159.5 (CO), 173.6 (CO).

(vii) 2-Carboxymethyl-5-hydroxybenzoic Acid (4d). 5-Amino-2-carboxymethylbenzoic acid **3** (1.00 g, 5.1 mmol) was dissolved at 5 °C in an aqueous sulfuric acid solution (3.0 mL of concentrated acid in 4.5 mL of water). A solution of sodium nitrite (0.534 g, 5.1 mmol) in water (3.0 mL) was slowly added while the temperature was kept below 5 °C to yield a pink solution of the diazonium salt. This diazonium mixture was added dropwise to a boiling aqueous sulfuric solution (1.0 mL of concentrated acid in 1.5 mL of water), and the solution was kept in an ice bath for 2 h. The precipitate was filtered, washed with distilled water, and dried at room temperature: beige solid; 47% yield; mp 212 °C; ^{1}H NMR (DMSO-d_6) δ 3.78 (s, 2H, CH_2), 6.87 (dd, 1H, ^3J = 8.2 Hz, ^4J = 2.4 Hz, H_4), 7.09 (d, 1H, ^3J = 8.2 Hz, H_3), 7.30 (d, 1H, ^4J = 2.4 Hz, H_6), 9.60 (s, 1H, OH); ^{13}C NMR (DMSO-d_6) δ 39.3 (CH_2), 115.7 (CH), 126.2 (C_2), 129.1 (CH), 131.6 (C_1), 154.3 (CO), 156.7 (C_5), 172.0 (CO).

Synthesis of Homophthalic Anhydrides (7a−c). (i) General Method. A solution of 5-amino-2-carboxymethylbenzoic acid **3** (1.00 g, 5.1 mmol) and acid chloride (39.0 mmol; acetyl chloride, valeroyl chloride, and benzoyl chloride for **7a**, **7b**, and **7c**, respectively) was refluxed for 90 min. After the mixture had cooled to room temperature, the formed crystals were filtered and rinsed with ether.

(ii) *N*-(1,3-Dioxo-3,4-dihydro-1*H*-isochromen-7-yl)acetamide (7a): salmon crystal; 99% yield; mp 197 °C; ^{1}H NMR (DMSO-d_6) δ 2.07 (s, 3H, CH_3), 4.19 (s, 2H, CH_2), 7.35 (d, 1H, ^3J = 8.5 Hz, H_5), 7.85 (dd, 1H, ^3J = 8.5 Hz, ^4J = 2.1 Hz, H_6), 8.37 (d, 1H, ^4J = 2.1 Hz, H_8), 10.30 (s, 1H, NH); ^{13}C NMR (DMSO-d_6) δ 23.9 (CH_3), 33.7 (CH_2), 118.8 (CH), 121.6 (C), 125.7 (C), 127.9 (CH), 130.8 (C), 138.6 (CH), 161.5 (CO), 165.4 (CO), 168.9 (CO).

(iii) *N*-(1,3-Dioxo-3,4-dihydro-1*H*-isochromen-7-yl)pentanamide (7b): yellow crystal; 95% yield; mp 202 °C; ^{1}H NMR (DMSO-d_6) δ 0.84 (t, 3H, ^3J = 7.5 Hz, CH_3), 1.29 (sext, 2H, ^3J = 7.3 Hz, $H_{3'}$), 1.56 (quin, 2H, ^3J = 7.5 Hz, $H_{2'}$), 2.35 (t, 2H, ^3J = 7.3 Hz, $H_{1'}$), 4.20 (s, 2H, CH_2), 7.34 (d, 1H, ^3J = 8.5 Hz, H_5), 7.88 (dd, 1H, ^3J = 8.5 Hz, ^4J = 2.1 Hz, H_6), 8.41 (d, 1H, ^4J = 2.1 Hz, H_8), 10.35 (s, 1H, NH); ^{13}C NMR (DMSO-d_6) δ 13.4 (CH_3), 21.5 (CH_2), 22.1 (CH_2), 26.8 (CH_2), 35.7 (CH_2), 118.5 (C), 121.2 (CH), 125.7 (C), 127.7 (CH), 130.2 (C), 138.6 (CH), 161.3 (CO), 165.5 (CO), 171.4 (CO).

(iv) *N*-(1,3-Dioxo-3,4-dihydro-1*H*-isochromen-7-yl)benzamide (7c): white crystal; 84% yield; mp 198 °C; ^{1}H NMR (DMSO-d_6) δ 4.24 (s, 2H, CH_2), 7.42 (d, 1H, ^3J = 8.4 Hz, H_5), 7.56 (m, 3H, HAr), 7.98 (d, 2H, $H_{6'}$, $H_{2'}$, ^3J = 6.4 Hz), 8.12 (dd, 1H, ^3J = 8.4 Hz, ^4J = 2.1 Hz, H_4), 8.56 (d, 1H, ^4J = 2.1 Hz, H_8), 10.56 (s, 1H, NH); ^{13}C NMR (DMSO-d_6) δ 33.8 (CH_2), 120.2 (CH), 121.7 (C), 126.9 (CH), 127.7 (2CH), 128.0 (CH), 128.5 (2CH), 131.4 (C), 131.9 (CH), 134.4 (C), 138.7 (C), 161.7 (CO), 165.8 (CO), 165.9 (CO).

Synthesis of the Homophthalic Acids (7d−g). (i) General Method. 5-Amino-2-carboxymethylbenzoic acid **3** (1.32 g, 6.8 mmol) was dissolved in 2.0 M KOH (20 mL). Then acid chloride (1.0 equiv) was added dropwise, and the solution was stirred for 2 h at room temperature. After acidification to pH 4.5 with aqueous 2.0 M HCl, the precipitate was filtered, washed three times with 1.0 M HCl (10 mL) and distilled water, and dried at room temperature.

(ii) 2-(Carboxymethyl)-5-{[(4-fluorophenyl)carbonyl]amino}-benzoic acid (7d): white solid; 86% yield; mp 278 °C; ^{1}H NMR (DMSO-d_6) δ 3.72 (s, 2H, CH_2), 7.22 (d, 1H, ^3J = 8.2 Hz, H_3), 7.36 (t, 2H, ^3J = 8.5 Hz, $H_{3'}$, $H_{5'}$), 7.86 (dd, 1H, ^3J = 8.2 Hz, ^4J = 2.0 Hz, H_4), 8.06 (dd, 2H, ^3J = 8.2 Hz, ^4J = 2.0 Hz, $H_{2'}$, $H_{6'}$), 8.15 (d, 1H, ^4J = 2.0 Hz, H_6), 10.35 (s, 1H, NH); ^{13}C NMR (DMSO-d_6) δ 41.4 (CH_2), 115.5 (d, 2CH, ^2J = 21.6 Hz, $C_{3'}$, $C_{5'}$), 122.6 (d, ^4J = 3.8 Hz, $C_{1'}$), 126.3 (CH), 127.5 (CH), 130.4 (d, 2CH, ^3J = 9.0 Hz, $C_{2'}$, $C_{6'}$), 131.3 (C), 131.4 (C), 135.0 (C), 137.8 (CH), 162.0 (d, ^1J = 247.0 Hz, $C_{4'}$), 162.8 (CO), 167.9 (CO), 171.2 (CO).

(iii) 2-(Carboxymethyl)-5-{[(3-nitrophenyl)carbonyl]amino}-benzoic acid (7e): white solid; 37% yield; mp 205 °C; ^{1}H NMR (DMSO-d_6) δ 3.90 (s, 2H, CH_2), 7.30 (d, 1H, ^3J = 8.0 Hz, H_3), 7.80 (m, 1H, HAr), 7.95 (dd, 1H, ^3J = 8.0 Hz, ^4J = 2.1 Hz, H_4), 8.38 (m, 3H, HAr), 8.80 (d, 1H, ^4J = 2.1 Hz, H_6), 10.80 (s, 1H, NH); ^{13}C NMR (DMSO-d_6) δ 36.6 (CH_2), 122.4 (CH), 122.5 (C), 123.6 (C), 128.1 (C), 130.1 (CH), 130.6 (CH), 132.1 (CH), 132.6 (C), 134.1 (CH), 137.8 (CH), 139.4 (CH), 147.6 (C), 163.2 (CO), 167.9 (CO), 172.5 (CO).

(iv) 2-(Carboxymethyl)-5-[(phenylacetyl)amino]benzoic acid (7f): white solid; 94% yield; mp 235 °C; ^{1}H NMR (DMSO-d_6) δ 3.64 (s, 2H, CH_2), 3.86 (s, 2H, CH_2), 7.22−7.34 (m, 6H, HAr), 7.73 (dd, 1H, ^3J = 8.5 Hz, ^4J = 2.0 Hz, H_4), 8.16 (d, 1H, ^4J = 2.0 Hz, H_6), 10.34 (s, 1H, NH); ^{13}C NMR (DMSO-d_6) δ 34.6 (CH_2), 37.0 (CH_2), 114.8 (C), 115.9 (C), 120.3 (CH), 122.0 (2CH), 123.0 (2CH), 124.4 (CH), 124.9 (CH), 126.4 (C), 129.5 (C), 131.7 (CH), 161.7 (CO), 163.0 (CO), 166.3 (CO).

(v) 2-(Carboxymethyl)-5-{[(4-fluorophenyl)acetyl]amino}benzoic acid (7g): white solid; 42% yield; mp 186 °C; ^{1}H NMR (DMSO-d_6) δ 3.63 (s, 2H, CH_2), 3.86 (s, 2H, CH_2), 7.15−7.35 (m, 5H, HAr), 7.70 (dd, 1H, ^3J = 8.5 Hz, ^4J = 2.0 Hz, H_4), 8.14 (d, 1H, ^4J = 2.0 Hz, H_6), 10.34 (s, 1H, NH); ^{13}C NMR (DMSO-d_6) δ 36.7 (CH_2), 42.4 (CH_2), 115.2 (d, 2CH, ^2J = 21.6 Hz, $C_{3'}$, $C_{5'}$), 121.1

(C), 122.4 (C), 130.9 (CH), 131.1 (d, 2CH, ^3J = 8.0 Hz, $C_{2'}$, $C_{6'}$), 131.5 (CH), 132.1 (d, ^4J = 3.0 Hz, $C_{1'}$), 132.9 (C), 138.1 (CH), 161.3 (d, ^1J = 250.0 Hz, $C_{4'}$), 168.2 (CO), 169.4 (CO), 172.7 (CO).

Synthesis of the Homophthalic Acids (7h−j). (i) General Method. A solution of 5-iodohomophthalic acid **4c** (0.36 g, 1.0 mmol), arylboronic acid (1.0 mmol), and $Pd(P\Phi_3)_4$ (30 mg) in benzene (3.0 mL) and aqueous 2.0 M K_2CO_3 (3.0 mL) was refluxed for 3 h. After the mixture had cooled, $CHCl_3$ (5.0 mL) and aqueous saturated $NaHCO_3$ (5.0 mL) were added. Insoluble materials were filtered. The aqueous layer was acidified with 1.0 M HCl and extracted with ethyl acetate. The organic layer was dried over Na_2SO_4 and concentrated in vacuo.

(ii) 2-Carboxymethyl-5-phenylbenzoic acid (7h): white solid; 76% yield; mp 220 °C; ^{1}H NMR (DMSO-d_6) δ 3.97 (s, 2H, CH_2), 7.39−7.54 (m, 2H, HAr), 7.70 (m, 2H, HAr), 7.80 (dd, 1H, ^3J = 8.0 Hz, ^4J = 2.0 Hz, H_4), 8.13 (m, 2H, HAr), 8.51 (d, 1H, ^3J = 8.2 Hz, H_6); ^{13}C NMR (DMSO-d_6) δ 39.7 (CH_2), 120.3 (CH), 126.0 (C_{IV}), 127.1 (CH), 128.8 (CH), 129.0 (2CH), 129.8 (CH), 130.1 (2CH), 134.1 (C_{IV}), 138.2 (C_{IV}), 139.5 (C_{IV}), 168.3 (CO), 172.4 (CO).

(iii) 2-Carboxymethyl-5-(4-methoxyphenyl)benzoic acid (7i): beige solid; 56% yield; mp 207 °C; ^{1}H NMR (DMSO-d_6) δ 3.85 (s, 3H, OMe), 4.09 (s, 2H, CH_2), 7.05 (d, 2H, ^3J = 9.0 Hz, HAr), 7.42 (d, 1H, ^3J = 8.0 Hz, H_3), 7.65 (d, 2H, ^3J = 9.0 Hz, HAr), 7.77 (dd, 1H, ^3J = 8.0 Hz, ^4J = 2.0 Hz, H_4), 8.26 (d, 1H, ^3J = 8.2 Hz, H_6); ^{13}C NMR (DMSO-d_6) δ 40.1 (CH_2), 55.7 (OMe), 115.3 (2CH), 128.8 (2CH), 129.2 (C_{IV}), 129.6 (CH), 130.7 (CH), 131.0 (C_{IV}), 131.5 (C_{IV}), 133.0 (C_{IV}), 133.9 (CH), 136.1 (C_{IV}), 168.7 (CO), 172.6 (CO).

(iv) 2-Carboxymethyl-5-(3,4-dimethoxyphenyl)benzoic acid (7j): black solid; 60% yield; mp 116 °C; ^{1}H NMR (DMSO-d_6) δ 3.82 (s, 3H, OMe), 3.88 (s, 3H, OMe), 4.06 (s, 2H, CH_2), 7.02 (d, 1H, ^3J = 8.5 Hz, $H_{5'}$), 7.20 (d, 1H, ^4J = 2.0 Hz, $H_{2'}$), 7.24 (dd, 1H, ^3J = 8.5 Hz, ^4J = 2.0 Hz, $H_{6'}$), 7.39 (d, 1H, ^3J = 8.0 Hz, H_3), 7.74 (dd, 1H, ^3J = 8.0 Hz, ^4J = 2.0 Hz, H_4), 8.23 (d, 1H, ^4J = 2.0 Hz, H_6); ^{13}C NMR (DMSO-d_6) δ 39.6 (CH_2), 55.8 (OMe), 55.9 (OMe), 106.7 ($C_{2'}$), 115.5 ($C_{5'}$), 123.0 (CH), 127.0 (CH), 127.6 (CH), 129.6 (CH), 130.1 (C_{IV}), 134.3 (C_{IV}), 138.6 (C_{IV}), 140.7 (C_{IV}), 149.1 ($C_{3'}$), 152.1 ($C_{4'}$), 168.7 (CO), 172.6 (CO).

Synthesis of 2-Benzyloxyisoquinoline-1,3(2*H*,4*H*)-dione Derivatives. (i) General Method. A solution of homophthalic acids or anhydrides (1.3 mmol) and *O*-benzylhydroxylamine (1.6 mmol; obtained from its hydrochloride salt) in toluene (250 mL) was refluxed using a Dean−Stark apparatus. Reaction was followed by TLC analysis (approximately 12 h). The hot solution was filtered and concentrated under reduced pressure. The residue was purified by column chromatography with hexane and ethyl acetate (8/2 to 5/5, % v/v).

(ii) 2-Benzyloxyisoquinoline-1,3-(2*H*,4*H*)-dione (5a): keto form (100%); white solid; 85% yield; mp 144 °C; ^{1}H NMR (DMSO-d_6) δ 4.20 (s, 2H, H_4), 5.15 (s, 2H, CH_2), 7.25−7.62 (m, 7H, H_7, H_5, $H_{2'-6'}$), 7.70 (td, 1H, ^3J = 8.5 Hz, ^4J = 2.4 Hz, H_6), 8.25 (dd, 1H, ^3J = 8.5 Hz, ^4J = 2.4 Hz, H_8); ^{13}C NMR (DMSO-d_6) δ 37.5 (C_4), 78.3 (CH_2), 125.2 (C_{8a}), 127.3 (CH), 127.9 (CH), 128.4 ($C_{2'}$, $C_{6'}$), 128.9 (CH), 129.0 (C_{4a}), 129.8 ($C_{3'}$, $C_{5'}$), 133.2 (CH), 133.8 ($C_{1'}$), 133.9 (CH), 161.4 (CO), 165.7 (CO).

(iii) 2-Benzyloxy-7-nitroisoquinoline-1,3(2*H*,4*H*)-dione (5b): keto form (100%); red solid; 60% yield; mp 236 °C; ^{1}H NMR (DMSO-d_6) δ 4.44 (s, 2H, H_4), 5.06 (s, 2H, CH_2), 7.42 (m, 3H, $H_{2'-6'}$), 7.59 (m, 2H, $H_{2'-6'}$), 7.72 (d, 1H, ^3J = 8.5 Hz, H_5), 8.50 (dd, 1H, ^3J = 8.5 Hz, ^4J = 2.4 Hz, H_6), 8.71 (d, 1H, ^4J = 2.4 Hz, H_8); ^{13}C NMR (DMSO-d_6) δ 36.9 (C_4), 76.7 (CH_2), 122.1 (CH), 126.4 (C_{IV}), 127.3 (CH), 128.2 ($C_{2'}$, $C_{6'}$), 128.7 (C_{IV}), 129.2 ($C_{3'}$, $C_{5'}$), 129.5 (CH), 134.3 (CH), 142.0 (C_{IV}), 146.3 (C_7), 159.6 (CO), 164.8 (CO).

(iv) 7-Amino-2-benzyloxyisoquinoline-1,3(2*H*,4*H*)-dione (5c): keto form (100%); yellow solid; 70% yield; mp 171 °C; ^{1}H NMR (DMSO-d_6) δ 4.07 (s, 2H, H_4), 5.00 (s, 2H, CH_2), 6.88 (dd, 1H, ^3J = 8.5 Hz, ^4J = 2.4 Hz, H_6), 7.04 (d, 1H, ^3J = 8.5 Hz, H_5), 7.24 (d, 1H, ^4J = 2.4 Hz, H_8), 7.39−7.57 (m, 5H, $H_{2'-6'}$); ^{13}C NMR (DMSO-d_6) δ 36.6 (C_4), 77.2 (CH_2), 111.2 (CH), 120.4 (CH), 121.2 (C_{IV}), 125.3 (C_{IV}), 128.4 ($C_{2'}$, $C_{6'}$), 128.8 (CH), 129.3 ($C_{3'}$, $C_{5'}$), 130.2 (C_{IV}), 134.7 (CH), 147.9 (C_7), 161.7 (CO), 166.6 (CO).

(v) 2-Benzyloxy-7-chloroisoquinoline-1,3(2*H*,4*H*)-dione (5d): keto form (100%); brown solid; 65% yield; mp 160 °C; ^{1}H NMR (DMSO-d_6) δ 4.27 (s, 2H, H_4), 5.03 (s, 2H, CH_2), 7.40−7.56 (m, 6H, H_5, $H_{2'-6'}$), 7.76 (dd, 1H, ^3J = 8.0 Hz, ^4J = 2.4 Hz, H_6), 8.00 (d, 1H, ^4J = 2.4 Hz, H_8); ^{13}C NMR (DMSO-d_6) δ 37.1 (C_4), 77.4 (CH_2), 126.8 (C_8), 127.0 (C_{8a}), 128.4 ($C_{2'}$, $C_{6'}$), 128.8 ($C_{4'}$), 129.4 ($C_{3'}$, $C_{5'}$), 130.0 (C_5), 132.1 (C_7), 133.4 ($C_{1'}$), 134.0 (C_{4a}), 134.6 (C_6), 160.4 (CO), 165.7 (CO).

(vi) 2-Benzyloxy-7-bromoisoquinoline-1,3(2*H*,4*H*)-dione (5e): keto form (100%); brown solid; 66% yield; mp 170 °C; ^{1}H NMR (DMSO-d_6) δ 4.24 (s, 2H, H_4), 5.02 (s, 2H, CH_2), 7.41 (m, 4H, $H_{2'-6'}$), 7.55 (m, 2H, H_5, $H_{2'-6'}$), 7.88 (dd, 1H, ^3J = 8.2 Hz, ^4J = 2.4 Hz, H_6), 8.12 (d, 1H, ^4J = 2.4 Hz, H_8); ^{13}C NMR (DMSO-d_6) δ 37.1 (C_4), 77.3 (CH_2), 120.1 (C_7), 127.3 (C_{8a}), 128.4 ($C_{2'}$, $C_{6'}$), 128.8 ($C_{4'}$), 129.3 ($C_{3'}$, $C_{5'}$), 129.8 (C_8), 130.1 (C_5), 134.3 (C_{4a}), 134.5 ($C_{1'}$), 136.2 (C_6), 160.3 (CO), 165.7 (CO).

(vii) 2-Benzyloxy-7-iodoisoquinoline-1,3(2*H*,4*H*)-dione (5f): keto form (100%); white solid; 80% yield; mp 180 °C; ^{1}H NMR (DMSO-d_6) δ 4.22 (s, 2H, H_4), 5.01 (s, 2H, CH_2), 7.22 (d, 1H, ^3J = 8.2 Hz, H_5), 7.40−7.56 (m, 5H, $H_{2'-6'}$), 8.02 (dd, 1H, ^3J = 8.2 Hz, ^4J = 2.4 Hz, H_6), 8.29 (d, 1H, ^4J = 2.4 Hz, H_8); ^{13}C NMR (DMSO-d_6) δ 37.1 (C_4), 77.4 (CH_2), 91.8 (C_7), 127.3 (C_{8a}), 128.4 ($C_{2'}$, $C_{6'}$), 128.8 ($C_{4'}$), 129.3 ($C_{3'}$, $C_{5'}$), 130.1 (C_5), 134.5 ($C_{1'}$), 134.8 (C_{4a}), 135.4 (C_8), 143.1 (C_6), 160.4 (CO), 165.7 (CO).

(viii) 2-Benzyloxy-7-hydroxyisoquinoline-1,3(2*H*,4*H*)-dione (5g): keto form (100%); pink solid; 40% yield; mp 188 °C; ^{1}H NMR (DMSO-d_6) δ 4.15 (s, 2H, H_4), 5.01 (s, 2H, CH_2), 7.08 (dd, 1H, ^3J = 8.5 Hz, ^4J = 2.1 Hz, H_6), 7.22 (d, 1H, ^3J = 8.5 Hz, H_5), 7.40−7.58 (m, 6H, H_8, $H_{2'-6'}$), 9.92 (s, 1H, OH); ^{13}C NMR (DMSO-d_6) δ 36.6 (C_4), 77.3 (CH_2), 112.9 (C_8), 121.8 (C_6), 125.0 (C_{8a}), 128.4 ($C_{2'}$, $C_{6'}$), 128.5 (C_{4a}), 128.8 ($C_{4'}$), 129.1 (C_5), 129.4 ($C_{3'}$, $C_{5'}$), 134.7 ($C_{1'}$), 156.5 (C_7), 161.3 (CO), 166.3 (CO).

(ix) *N*-[2-(Benzyloxy)-1,3-dioxo-1,2,3,4-tetrahydroisoquinolin-7-yl]pentanamide (5i): keto form (100%); yellow solid; 72% yield; mp 179 °C; ^{1}H NMR (DMSO-d_6) δ 0.90 (t, 3H, ^3J = 7.5 Hz, CH_3), 1.33 (sext, 2H, ^3J = 8.5 Hz, ^4J = 2.5 Hz, $H_{3'}$), 1.59 (quint, 2H, ^3J = 7.3 Hz, $H_{2'}$), 2.34 (t, 2H, ^3J = 7.3 Hz, $H_{1'}$), 4.20 (s, 2H, CH_2), 7.31−7.42 (m, 4H, HAr), 7.55 (m, 2H, HAr), 7.88 (dd, 1H, ^3J = 8.5 Hz, ^4J = 2.5 Hz, H_6), 8.35 (d, 1H, ^4J = 2.2 Hz, H_8), 10.16 (s, 1H, NH); ^{13}C NMR (DMSO-d_6) δ 13.7 (CH_3), 21.8 (CH_2), 27.1 (CH_2), 36.1 (CH_2), 36.9 (CH_2), 77.3 (OCH_2), 117.4 (C), 124.4 (C), 125.3 (C), 128.1 (C), 128.3 (2C), 128.8 (CH), 129.0 (CH), 129.4 (2C), 134.6 (CH), 138.5 (CH), 161.3 (CO), 166.1 (CO), 171.6 (CO).

(x) *N*-[2-(Benzyloxy)-1,3-dioxo-1,2,3,4-tetrahydroisoquinolin-7-yl]benzamide (5j): keto form (100%); orange solid; 85% yield; mp 201 °C; ^{1}H NMR (DMSO-d_6) δ 4.26 (s, 2H, H_4), 5.06 (s, 2H, OCH_2), 7.75 (m, 9H, HAr), 8.00 (m, 3H, HAr), 8.55 (d, 1H, ^4J = 2.0 Hz, H_8), 10.56 (s, 1H, NH); ^{13}C NMR (DMSO-d_6) δ 37.3 (CH_2), 77.3 (OCH_2), 118.8 (C), 125.3 (CH), 125.6 (C), 128.3 (2CH), 128.4 (C), 128.8 (2CH), 129.2 (CH), 129.4 (2CH), 129.7 (CH), 131.8 (C), 134.5 (C), 134.7 (CH), 138.5 (CH), 161.3 (CO), 165.7 (CO), 166.1 (CO).

(xi) *N*-[2-(Benzyloxy)-1,3-dioxo-1,2,3,4-tetrahydroisoquinolin-7-yl]-4-fluorobenzamide (5k): keto form (100%); yellow solid; 15% yield; mp 218 °C; ^{1}H NMR (DMSO-d_6) δ 4.26 (s, 2H, H_4), 5.04 (s, 2H, OCH_2), 7.39 (m, 6H, HAr), 7.56 (m, 2H, HAr), 8.05 (m, 3H, HAr), 8.50 (d, 1H, ^4J = 2.0 Hz, H_8), 10.55 (s, 1H, NH); ^{13}C NMR (DMSO-d_6) δ 36.2 (CH_2), 78.0 (OCH_2), 115.7 (d, 2CH, ^2J = 21.0 Hz, $C_{3'}$, $C_{5'}$), 118.5 (C), 124.0 (C), 125.5 (d, ^4J = 3.0 Hz, $C_{1'}$), 128.5 (C), 129.0 (2CH), 129.8 (CH), 130.1 (2CH), 130.7 (CH), 130.9 (d, 2CH, ^3J = 8.0 Hz, $C_{2'}$, $C_{6'}$), 131.2 (C), 134.5 (CH), 138.5 (CH), 163.5 (d, ^1J = 250.0 Hz, $C_{4'}$), 163.9 (CO), 164.1 (CO), 164.7 (CO).

(xii) *N*-[2-(Benzyloxy)-1,3-dioxo-1,2,3,4-tetrahydroisoquinolin-7-yl]-3-nitrobenzamide (5l): keto form (100%); orange solid; 67% yield; mp 218 °C; ^{1}H NMR (DMSO-d_6) δ 4.34 (s, 2H, H_4), 5.12 (s, 2H, OCH_2), 7.42−7.53 (m, 4H, HAr), 7.61−7.67 (m, 2H, HAr), 7.93 (dd, 1H, ^3J = 8.2 Hz, ^4J = 2.1 Hz, HAr), 8.17 (dd, 1H, ^3J = 8.3 Hz, ^4J = 2.1 Hz, HAr), 8.51 (m, 2H, HAr), 8.59 (d, 1H, ^3J =

8.0 Hz, H_5), 8.92 (d, 1H, ^4J = 1.9 Hz, H_8), 10.92 (s, 1H, NH); ^{13}C NMR (DMSO-d_6) δ 39.5 (CH_2), 77.9 (OCH_2), 119.5 (CH), 123.0 (CH), 126.0 (C), 126.2 (CH), 127.0 (CH), 128.7 (CH), 128.9 (2CH), 129.3 (CH), 129.9 (2CH), 130.8 (CH), 138.0 (C), 134.8 (CH), 135.1 (C), 136.2 (C), 138.4 (C), 148.2 (C), 161.8 (CO), 164.0 (CO), 166.6 (CO).

(xiii) *N*-[2-(Benzyloxy)-1,3-dioxo-1,2,3,4-tetrahydroisoquinolin-7-yl]-2-phenylacetamide (5m): keto form (100%); brown solid; 57% yield; mp 217 °C; ^{1}H NMR (DMSO-d_6) δ 3.67 (s, 2H, CH_2), 4.21 (s, 2H, H_4), 5.02 (s, 2H, OCH_2), 7.35 (m, 9H, HAr), 7.55 (m, 2H, HAr), 7.56 (dd, 1H, ^3J = 8.5 Hz, ^4J = 1.5 Hz, H_6), 8.35 (d, 1H, ^4J = 1.5 Hz, H_8), 10.47 (s, 1H, NH); ^{13}C NMR (DMSO-d_6) δ 36.9 (CH_2), 43.3 (CH_2), 77.3 (OCH_2), 117.5 (C), 124.5 (C), 125.4 (C), 126.5 (C), 126.6 (CH), 128.3 (CH), 128.4 (2CH), 128.6 (CH), 129.0 (2CH), 129.1 (2CH), 129.3 (2CH), 134.6 (CH), 135.7 (CH), 138.4 (C), 161.2 (CO), 166.1 (CO), 169.4 (CO).

(xiv) *N*-[2-(Benzyloxy)-1,3-dioxo-1,2,3,4-tetrahydroisoquinolin-7-yl]-2-(4-fluorophenyl)acetamide (5n): keto form (100%); white solid; 9% yield; mp 221 °C; ^{1}H NMR (DMSO-d_6) δ 3.67 (s, 2H, CH_2), 4.21 (s, 2H, H_4), 5.02 (s, 2H, OCH_2), 7.16 (t, 2H, ^3J = 8.2 Hz, HAr), 7.37 (m, 7H, HAr), 7.55 (m, 2H, HAr), 7.84 (dd, 1H, ^3J = 8.0 Hz, ^4J = 2.0 Hz, H_6), 10.46 (s, 1H, NH); ^{13}C NMR (DMSO-d_6) δ 36.6 (CH_2), 43.0 (CH_2), 77.5 (OCH_2), 115.0 (d, 2CH, ^2J = 21.6 Hz, $C_{3'}$, $C_{5'}$), 117.5 (C), 119.2 (d, ^4J = 3.0 Hz, $C_{1'}$), 124.2 (C), 125.3 (CH), 128.0 (2CH), 128.2 (C), 129.1 (CH), 130.2 (2CH), 131.0 (d, 2CH, ^3J = 8.0 Hz, $C_{2'}$, $C_{6'}$), 131.9 (C), 138.1 (CH), 138.3 (CH), 161.1 (d, ^1J = 250.0 Hz, $C_{4'}$), 161.6 (CO), 166.3 (CO), 169.3 (CO).

(xv) 2-(Benzyloxy)-7-(4-fluorophenyl)isoquinoline-1,3(2*H*,4*H*)-dione (5o): keto form (100%); brown solid; 60% yield; mp 180 °C; ^{1}H NMR (DMSO-d_6) δ 4.32 (s, 2H, H_4), 5.20 (s, 2H, OCH_2), 7.33−7.43 (m, 5H, HAr), 7.64 (m, 2H, HAr), 7.96 (d, 2H, ^3J = 7.5 Hz), 8.24 (m, 2H, HAr), 8.51 (d, 1H, ^4J = 2.0 Hz, H_8); ^{13}C NMR (DMSO-d_6) δ 36.9 (C_4), 77.4 (CH_2), 116.0 (d, ^2J = 21.4 Hz, $C_{3''}$, $C_{5''}$), 125.3 (CH), 125.6 (C), 128.4 (CH), 128.5 ($C_{2'}$, $C_{6'}$), 128.8 (CH), 128.9 (d, ^3J = 8.0 Hz, $C_{2''}$, $C_{6''}$), 129.2 ($C_{3'}$, $C_{5'}$), 131.6 (CH), 133.7 (C), 133.8 (C), 135.2 (d, ^4J = 3.2 Hz, $C_{1''}$), 138.2 (C), 161.7 (CO), 162.5 (d, ^1J = 243.5 Hz, $C_{4''}$), 166.3 (CO).

(xvi) 2-Benzyloxy-7-[4-(trifluoromethyl)phenyl]isoquinoline-1,3(2*H*,4*H*)-dione (5p): keto form (100%); light brown solid; 32% yield; mp 200 °C; ^{1}H NMR (acetone-d_6) δ 4.35 (s, 2H, H_4), 5.14 (s, 2H, OCH_2), 7.40−7.58 (m, 3H, HAr), 7.62−7.64 (m, 3H, HAr), 7.84 (d, 2H, ^3J = 7.6 Hz, HAr), 7.98−8.08 (m, 3H, HAr), 8.43 (d, 1H, ^4J = 2.0 Hz, H_8); ^{13}C NMR (acetone-d_6) δ 37.9 (C_4), 77.3 (CH_2), 125.4 (q, ^1J = 270.0 Hz, CF_3), 126.8 (q, ^3J = 4.0 Hz, $C_{3''}$, $C_{5''}$), 127.1 (CH), 128.4 (C), 128.5 (2CH), 128.6 (2CH), 128.8 (CH), 129.2 (2CH), 129.6 (CH), 130.2 (q, ^2J = 33.0 Hz, $C_{4''}$), 132.9 (CH), 134.5 (C), 135.4 (C), 139.5 (C), 144.2 (C), 161.8 (CO), 166.1 (CO).

(xvii) 2-Benzyloxy-7-phenylisoquinoline-1,3(2*H*,4*H*)-dione (5q): keto form (100%); light yellow solid; 98% yield; mp 202 °C; ^{1}H NMR (DMSO-d_6) δ 4.17 (s, 2H, H_4), 5.02 (s, 2H, OCH_2), 7.20−7.26 (m, 11H, HAr), 7.84 (dd, 1H, ^3J = 8.0 Hz, ^4J = 2.0 Hz, H_6), 8.45 (d, 1H, ^4J = 2.0 Hz, H_8); ^{13}C NMR (DMSO-d_6) δ 31.1 (C_4), 77.5 (OCH_2), 119.5 (C), 120.8 (2CH), 121.1 (CH), 121.7 (CH), 121.9 (CH), 122.2 (2CH), 122.8 (2CH), 122.9 (2CH), 123.7 (2CH), 125.7 (C), 126.3 (CH), 127.7 (C), 132.8 (C), 134.9 (C), 155.3 (CO), 159.5 (CO).

(xviii) 2-Benzyloxy-7-(4-methoxyphenyl)isoquinoline-1,3(2*H*,4*H*)-dione (5r): keto form (100%); orange solid; 40% yield; mp 205 °C; ^{1}H NMR (DMSO-d_6) δ 3.85 (s, 3H, CH_3), 4.13 (s, 2H, H_4), 5.14 (s, 2H, OCH_2), 6.98 (d, 2H, ^3J = 8.0 Hz, HAr), 7.28−7.39 (m, 4H, HAr), 7.54−7.60 (m, 4H, HAr), 7.78 (dd, 1H, ^3J = 8.0 Hz, ^4J = 2.0 Hz, H_6), 8.38 (d, 1H, ^4J = 2.0 Hz, H_8); ^{13}C NMR (DMSO-d_6) δ 37.1 (C_4), 55.7 (OCH_3), 77.5 (OCH_2), 115.3 (2CH), 128.5 (2CH), 128.7 (CH), 128.8 (2CH), 129.0 (2CH), 129.2 (C), 129.6 (CH), 130.7 (CH), 131.0 (C), 131.5 (C), 133.0 (C), 133.9 (CH), 134.5 (C), 136.1 (C), 168.7 (CO), 172.6 (CO).

(xix) 2-Benzyloxy-7-(3,4-dimethoxyphenyl)isoquinoline-1,3(2*H*,4*H*)-dione (5s): keto form (100%); orange solid; 22% yield; mp 122 °C; ^{1}H NMR (DMSO-d_6) δ 3.94 (s, 3H, CH_3), 3.98 (s, 3H, CH_3), 4.17 (s, 2H, H_4), 5.16 (s, 2H, OCH_2), 6.98 (d, 1H, ^3J = 8.5 Hz, $H_{5''}$), 7.14 (dd, 1H, ^3J = 8.5 Hz, ^4J = 2.0 Hz, $H_{6''}$), 7.20 (d, 1H, ^4J = 2.0 Hz, $H_{2''}$), 7.31−7.41 (m, 4H, HAr), 7.59−7.62 (m, 2H, HAr), 7.80 (dd, 1H, ^3J = 8.0 Hz, ^4J = 2.0 Hz, H_6), 8.41 (d, 1H, ^4J = 2.0 Hz, H_8); ^{13}C NMR (DMSO-d_6) δ 37.1 (C_4), 55.8 (OCH_3), 55.9 (OCH_3), 77.4 (OCH_2), 106.8 ($C_{5''}$), 114.5 ($C_{2''}$), 123.0 (CH), 127.0 (CH), 128.5 (2CH), 128.8 (CH), 129.2 (2CH), 129.6 (CH), 130.1 (C), 131.1 (CH), 134.0 (C), 134.4 (C), 135.2 (C), 142.7 (C), 147.2 ($C_{3''}$), 152.1 ($C_{4''}$), 161.6 (CO), 165.5 (CO).

Synthesis of 2-Hydroxyisoquinoline-1,3(2*H*,4*H*)-dione Derivatives. (i) General Method. 2-Benzyloxyisoquinoline-1,3(2*H*,4*H*)-dione derivatives (1.9 mmol) were dissolved in a minimum amount of CH_2Cl_2, and boron tribromide (1.0 M solution in CH_2Cl_2, 7.5 mL, 7.5 mmol) was added dropwise at room temperature. The solution was stirred for 1 h, and water (20 mL) was slowly added. After the mixture had been stirred for 15 min, the precipitate was filtered and the aqueous layer was extracted with ethyl acetate. Organic layers were dried over Na_2SO_4 and concentrated in vacuo. Organic residues and precipitate were gathered, and 2-hydroxyisoquinoline-1,3(2*H*,4*H*)-dione derivatives were obtained after recrystallization in an appropriate solvent (mostly butanone or ethanol).

(ii) 2-Hydroxyisoquinoline-1,3(2*H*,4*H*)-dione (6a): recrystallization solvent, butanone; keto form (100%); orange solid; 86% yield; mp 199 °C; ^{1}H NMR (DMSO-d_6) δ 4.26 (s, 2H, H_4), 7.37−7.52 (m, 2H, H_7, H_5), 7.70 (td, 1H, ^3J = 7.6 Hz, ^4J = 1.5 Hz, H_6), 8.03 (dd, 1H, ^3J = 7.6 Hz, ^4J = 1.5 Hz, H_8), 10.4 (s, 1H, OH); ^{13}C NMR (DMSO-d_6) δ 37.6 (C_4), 125.6 (C_{8a}), 125.8 (C_7), 126.5 (C_8), 128.4 (C_5), 131.8 (C_6), 135.7 (C_{4a}), 161.3 (C_1), 166.0 (C_3); ESI-MS *m*/*z* 178 $(M + H)^+$. Anal. ($C_9H_7NO_3$) C, H, N.

(iii) 2-Hydroxy-7-nitroisoquinoline-1,3(2*H*,4*H*)-dione (6b): keto form (70%); brown solid; 55% yield; mp 226 °C; ^{1}H NMR (DMSO-d_6) δ 4.41 (s, 2H, H_4), 7.68 (d, 1H, ^3J = 8.0 Hz, H_5), 8.45 (dd, 1H, ^3J = 8.0 Hz, ^4J = 2.4 Hz, H_6), 8.66 (d, 1H, ^4J = 2.4 Hz, H_8), 10.4 (s, 1H, OH); ^{13}C NMR (DMSO-d_6) δ 36.4 (C_4), 121.4 (C_8), 126.4 (C_{8a}), 127.8 (C_6), 129.3 (C_5), 141.6 (C_{4a}), 145.6 (C_7), 161.2 (C_1), 164.7 (C_3); ESI-MS *m*/*z* 223 $(M + H)^+$. Anal. ($C_9H_6N_2O_5$) C, H, N.

(iv) 7-Amino-2-hydroxyisoquinoline-1,3(2*H*,4*H*)-dione (6c): keto form (100%); brown solid; 35% yield; mp 180 °C; ^{1}H NMR (DMSO-d_6) δ 4.03 (s, 2H, H_4), 6.85 (dd, 1H, ^3J = 8.2 Hz, ^4J = 2.4 Hz, H_6), 7.02 (d, 1H, ^3J = 8.2 Hz, H_5), 7.21 (d, 1H, ^4J = 2.1 Hz, H_8), 10.26 (s, 1H, OH); ^{13}C NMR (DMSO-d_6) δ 36.6 (C_4), 111.1 (C_8), 119.8 (C_6), 120.9 (C_{4a}), 125.3 (C_{8a}), 128.1 (C_5), 148.0 (C_7), 162.2 (C_1), 166.8 (C_3); ESI-MS *m*/*z* 193 $(M + H)^+$. Anal. ($C_9H_8N_2O_3$) C, H, N.

(v) 7-Chloro-2-hydroxyisoquinoline-1,3(2*H*,4*H*)-dione (6d): recrystallization solvent, butanone; keto form (90%); transparent crystals; 75% yield; mp 216 °C; ^{1}H NMR (DMSO-d_6) δ 4.25 (s, 2H, H_4), 7.44 (d, 1H, ^3J = 8.2 Hz, H_5), 7.72 (dd, 1H, ^3J = 8.2 Hz, ^4J = 2.4 Hz, H_6), 7.96 (d, 1H, ^4J = 2.4 Hz, H_8), 9.58 (s, 1H, OH); ^{13}C NMR (DMSO-d_6) δ 36.5 (C_4), 126.7 (C_8), 126.9 (C_{8a}), 129.8 (C_5), 132.0 (C_7), 133.1 (C_6), 133.6 (C_{4a}), 160.7 (C_1), 165.9 (C_3); ESI-MS *m*/*z* 212 $(M + H)^+$. Anal. ($C_9H_6ClNO_3$) C, H, N.

(vi) 7-Bromo-2-hydroxyisoquinoline-1,3(2*H*,4*H*)-dione (6e): keto form (90%); orange solid; 50% yield; mp 180 °C; ^{1}H NMR (DMSO-d_6) δ 4.41 (s, 2H, H_4), 7.90 (d, 1H, ^3J = 8.2 Hz, H_5), 8.30 (dd, 1H, ^3J = 8.0 Hz, ^4J = 2.4 Hz, H_6), 8.66 (d, 1H, ^4J = 2.4 Hz, H_8), 10.04 (s, 1H, OH); ^{13}C NMR (DMSO-d_6) δ 36.6 (C_4), 120.0 (C_7), 127.2 (C_{8a}), 129.6 (C_8), 130.0 (C_5), 134.1 (C_{4a}), 135.9 (C_6), 160.6 (C_1), 166.0 (C_3); ESI-MS *m*/*z* 257 $(M + H)^+$. Anal. ($C_9H_6BrNO_3$) C, H, N.

(vii) 2-Hydroxy-7-iodoisoquinoline-1,3(2*H*,4*H*)-dione (6f): keto form (95%); brown solid; 60% yield; mp 190 °C; ^{1}H NMR (DMSO-d_6) δ 4.22 (s, 2H, H_4), 7.28 (d, 1H, ^3J = 8.0 Hz, H_5), 8.00 (dd, 1H, ^3J = 8.0 Hz, ^4J = 2.4 Hz, H_6), 8.39 (d, 1H, ^4J = 2.4 Hz, H_8), 9.53 (s, 1H, OH); ^{13}C NMR (DMSO-d_6) δ 36.6 (C_4), 91.7 (C_7), 127.2 (C_{8a}), 130.0 (C_5), 134.5 (C_{4a}), 135.2 (C_8), 142.7 (C_6), 160.7 (C_1), 166.0 (C_3); ESI-MS *m*/*z* 300 $(M + H)^+$. Anal. ($C_9H_6INO_3$) C, H, N.

(viii) 2,7-Dihydroxyisoquinoline-1,3(2*H*,4*H*)-dione (6g): keto form (100%); light brown solid; 47% yield; mp 220 °C; ^{1}H NMR (DMSO-d_6) δ 4.12 (s, 2H, H_4), 7.06 (dd, 1H, ^3J = 8.2 Hz, ^4J =

2.4 Hz, H_6), 7.20 (d, 1H, ^4J = 8.2 Hz, H_5), 7.38 (d, 1H, ^4J = 2.4 Hz, H_8), 9.88 (s, 1H, OH); ^{13}C NMR (DMSO-d_6) δ 36.1 (C_4), 112.8 (C_6), 121.4 (C_{8a}), 124.7 (C_8), 125.8 (C_{4a}), 128.9 (C_5), 156.4 (C_7), 161.7 (C_1), 166.5 (C_3); ESI-MS *m/z* 194 (M + H)$^+$. Anal. ($C_9H_7NO_4$) C, H, N.

(ix) *N*-(2-Hydroxy-1,3-dioxo-1,2,3,4-tetrahydroisoquinolin-7-yl)acetamide (6h). Na_2CO_3 (0.12 g, 1.1 mmol) and hydroxylamine hydrochloride (0.16 g, 2.3 mmol) were dissolved in distilled water (0.7 mL). A solution of *N*-(1,3-dioxo-3,4-dihydro-1*H*-isochromen-7-yl)acetamide **7a** (0.5 g, 2.3 mmol) in distilled water (7.0 mL) was added dropwise, and the solution was refluxed for 15 min. After the mixture had cooled to room temperature, the precipitate was filtered and rinsed with ether: orange solid; 65% yield; mp 189 °C; ^{1}H NMR (DMSO-d_6) δ 2.06 (s, 3H, CH_3), 4.18 (s, 2H, H_4), 7.30 (d, 1H, ^3J = 8.5 Hz, H_5), 7.80 (dd, 1H, ^3J = 8.5 Hz, ^4J = 2.1 Hz, H_6), 8.31 (d, 1H, ^4J = 2.1 Hz, H_8), 10.22 (s, 1H, NH), 10.40 (s, 1H, OH); ^{13}C NMR (DMSO-d_6) δ 24.0 (CH_3), 36.4 (C_4), 117.2 (CH), 124.0 (CH), 125.3 (C), 128.1 (CH), 128.8 (C), 138.5 (C), 161.7 (CO), 166.4 (CO), 168.6 (CO); ESI-MS *m/z* 235 (M + H)$^+$ (20), 218 (10), 207 (90), 175 (10), 162 (20), 147 (100). Anal. ($C_{11}H_{10}N_2O_4$) C, H, N.

(x) *N*-(2-Hydroxy-1,3-dioxo-1,2,3,4-tetrahydroisoquinolin-7-yl)pentanamide (6i): treatment with boron tribromide (4 equiv); orange solid; 90% yield; mp 179 °C; ^{1}H NMR (DMSO-d_6) δ 0.89 (t, 3H, ^3J = 7.3 Hz, CH_3), 1.32 (sext, 2H, ^3J = 7.6 Hz, $H_{4'}$), 1.55 (quin, 2H, ^3J = 7.3 Hz, $H_{3'}$), 2.32 (t, 2H, ^3J = 7.3 Hz, $H_{2'}$), 4.18 (s, 2H, CH_2), 7.30 (d, 1H, ^3J = 8.5 Hz, H_5), 7.81 (dd, 1H, ^3J = 8.5 Hz, ^4J = 1.8 Hz, H_6), 8.33 (d, 1H, ^4J = 1.8 Hz, H_8), 10.15 (s, 1H, NH); ^{13}C NMR (DMSO-d_6) δ 13.7 (CH_3), 21.8 (CH_2), 27.2 (CH_2), 36.1 (CH_2), 36.4 (CH_2), 117.4 (C), 124.2 (C), 125.3 (C), 128.1 (CH), 128.8 (CH), 138.5 (CH), 161.7 (CO), 166.4 (CO), 171.6 (CO); ESI-MS *m/z* 277 (M + H)$^+$. Anal. ($C_{14}H_{16}N_2O_4$) C, H, N.

(xi) *N*-(2-Hydroxy-1,3-dioxo-1,2,3,4-tetrahydroisoquinolin-7-yl)benzamide (6j): treatment with boron tribromide (5 equiv); light pink solid; 65% yield; mp 175 °C; ^{1}H NMR (DMSO-d_6) δ 4.18 (s, 2H, H_4), 7.30−7.57 (m, 4H, HAr), 8.00 (m, 2H, HAr), 8.15 (dd, 1H, ^3J = 8.2 Hz, ^4J = 2.0 Hz, H_6), 8.54 (d, 1H, ^4J = 2.0 Hz, H_8), 10.50 (s, 1H, NH); ^{13}C NMR (DMSO-d_6) δ 36.4 (C_4), 118.7 (CH), 125.2 (C), 125.3 (CH), 127.6 (2CH), 128.0 (CH), 128.4 (2CH), 129.5 (C), 131.7 (CH), 134.4 (C), 138.3 (C), 161.6 (CO), 165.6 (CO), 166.3 (CO); ESI-MS *m/z* 297 (M + H)$^+$ (10), 269 (50), 224 (10), 105 (100). Anal. ($C_{16}H_{12}N_2O_4$) C, H, N.

(xii) *N*-(2-Hydroxy-1,3-dioxo-1,2,3,4-tetrahydroisoquinolin-7-yl)-4-fluorobenzamide (6k): treatment with boron tribromide (5 equiv); yellow solid; 54% yield; mp 232 °C; ^{1}H NMR (DMSO-d_6) δ 4.22 (s, 2H, H_4), 7.38 (m, 3H, HAr), 8.07 (m, 3H, HAr), 8.48 (d, 1H, ^4J = 2.0 Hz, H_8), 10.50 (s, 1H, NH); ^{13}C NMR (DMSO-d_6) δ 36.7 (C_4), 115.5 (d, ^2J = 21.0 Hz, $C_{3'}$, $C_{5'}$), 119.0 (C), 125.5 (d, ^4J = 3.0 Hz, $C_{1'}$), 128.4 (C), 129.8 (CH), 130.6 (CH), 130.9 (d, ^3J = 8.0 Hz, $C_{2'}$, $C_{6'}$), 131.2 (C), 138.5 (CH), 163.5 (d, ^1J = 250.0 Hz, $C_{4'}$), 164.7 (CO), 166.6 (CO), 167.0 (CO); ESI-MS *m/z* 315 (M + H)$^+$ (10), 287 (60), 242 (10), 123 (100). Anal. ($C_{16}H_{11}FN_2O_4$) C, H, N.

(xiii) *N*-(2-Hydroxy-1,3-dioxo-1,2,3,4-tetrahydroisoquinolin-7-yl)-3-nitrobenzamide (6l): treatment with boron tribromide (5 equiv); keto form (97%); yellow solid; 95% yield; mp 188 °C; ^{1}H NMR (DMSO-d_6) δ 4.25 (s, 2H, H_4), 7.41 (d, 1H, ^3J = 8.0 Hz, H_5), 7.86 (t, 1H, ^3J = 8.0 Hz, $H_{5'}$), 8.10 (dd, 1H, ^3J = 8.1 Hz, ^4J = 2.0 Hz, HAr), 8.45 (m, 2H, HAr), 8.50 (d, 1H, ^4J = 2.0 Hz, HAr), 8.85 (d, 1H, ^4J = 2.0 Hz, HAr), 10.83 (s, 1H, NH); ^{13}C NMR (DMSO-d_6) δ 37.2 (C_4), 119.4 (CH), 123.0 (CH), 125.9 (C), 126.0 (CH), 126.9 (CH), 128.3 (CH), 130.6 (C), 130.8 (CH), 134.7 (CH), 138.4 (C), 147.7 (C), 148.2 (C), 162.2 (CO), 164.1 (CO), 167.0 (CO); ESI-MS *m/z* 342 (M + H)$^+$. Anal. ($C_{16}H_{11}N_3O_6$) C, H, N.

(xiv) *N*-(2-Hydroxy-1,3-dioxo-1,2,3,4-tetrahydroisoquinolin-7-yl)-2-phenylacetamide (6m): brown solid; 86% yield; mp 188 °C; ^{1}H NMR (DMSO-d_6) δ 3.66 (s, 2H, CH_2), 4.18 (s, 2H, H_4), 7.33 (m, 6H, HAr), 7.84 (dd, 1H, ^3J = 8.0 Hz, ^4J = 1.5 Hz, H_6), 8.33 (d, 1H, ^4J = 1.5 Hz, H_8), 10.47 (s, 1H, NH); ^{13}C NMR (DMSO-d_6) δ 36.6 (CH_2), 43.4 (CH_2), 117.6 (C), 124.4 (C), 125.4 (C), 126.8 (CH), 128.4 (CH), 128.5 (2CH), 129.3 (2CH), 129.4 (CH), 135.8 (C), 138.4 (CH), 161.8 (CO), 166.6 (CO), 169.7 (CO); ESI-MS *m/z* 311 (M + H)$^+$ (30), 283 (100), 238 (30), 147 (100), 91 (30). Anal. ($C_{17}H_{14}N_2O_4$) C, H, N.

(xv) 2-(4-Fluorophenyl)-*N*-(2-hydroxy-1,3-dioxo-1,2,3,4-tetrahydroisoquinolin-7-yl)acetamide (6n): light yellow solid; 55% yield; mp 210 °C; ^{1}H NMR (DMSO-d_6) δ 3.66 (s, 2H, CH_2), 4.19 (s, 2H, H_4), 7.15 (t, 2H, ^3J = 8.2 Hz, HAr), 7.37 (m, 3H, HAr), 7.82 (dd, 1H, ^3J = 8.2 Hz, ^4J = 1.8 Hz, H_6), 8.32 (d, 1H, ^4J = 1.8 Hz, H_8), 10.43 (s, 1H, NH); ^{13}C NMR (DMSO-d_6) δ 36.4 (CH_2), 42.2 (CH_2), 115.0 (d, 2CH, ^2J = 21.6 Hz, $C_{3'}$, $C_{5'}$), 117.5 (d, ^4J = 3.0 Hz, $C_{1'}$), 124.2 (C), 125.3 (CH), 128.2 (C), 129.1 (CH), 131.0 (d, 2CH, ^3J = 8.0 Hz, $C_{2'}$, $C_{6'}$), 131.9 (C), 138.3 (CH), 161.1 (d, ^1J = 250.0 Hz, $C_{4'}$), 161.6 (CO), 166.3 (CO), 169.3 (CO); ESI-MS *m/z* 329 (M + H)$^+$ (20), 301 (80), 256 (20), 147 (100), 109 (30). Anal. ($C_{17}H_{13}FN_2O_4$) C, H, N.

(xvi) 7-(4-Fluorophenyl)-2-hydroxyisoquinoline-1,3(2*H*,4*H*)-dione (6o): keto form (100%); beige solid; 47% yield; mp 175 °C; ^{1}H NMR (DMSO-d_6) δ 4.30 (s, 2H, H_4), 7.32 (t, 2H, ^3J = 8.8 Hz, $H_{3'}$, $H_{5'}$), 7.48 (d, 1H, ^3J = 8.0 Hz, H_5), 7.78 (dd, 2H, ^3J = 8.8 Hz, ^4J = 5.0 Hz, $H_{2'}$, $H_{6'}$), 7.94 (dd, 1H, ^3J = 8.0 Hz, ^4J = 1.5 Hz, H_6), 8.21 (d, 1H, ^4J = 1.5 Hz, H_8), 10.45 (s, 1H, OH); ^{13}C NMR (DMSO-d_6) δ 36.7 (C_4), 115.9 (d, ^2J = 21.5 Hz, $C_{3'}$, $C_{5'}$), 125.2 (CH), 125.6 (C), 128.5 (CH), 128.8 (d, ^3J = 8.2 Hz, $C_{2'}$, $C_{6'}$), 131.6 (CH), 133.7 (C), 135.2 (d, ^4J = 3.0 Hz, $C_{1'}$), 138.2 (C), 161.7 (CO), 166.3 (CO); ESI-MS *m/z* 272 (M + H)$^+$. Anal. ($C_{15}H_{10}FNO_3$) C, H, N.

(xvii) 2-Hydroxy-7-[4-(trifluoromethyl)phenyl]isoquinoline-1,3(2*H*,4*H*)-dione (6p): keto form (100%); brown solid; 45% yield; mp 209 °C; ^{1}H NMR (acetone-d_6) δ 4.33 (s, 2H, H_4), 7.60 (d, 1H, ^3J = 8.5 Hz, H_5), 7.86 (d, 2H, HAr), 7.97−8.06 (m, 3H, HAr), 8.40 (d, 1H, ^4J = 2.0 Hz, H_8), 9.53 (s, 1H, OH); ^{13}C NMR (acetone-d_6) δ 37.4 (C_4), 126.8 (q, ^3J = 4.0 Hz, $C_{3'}$, $C_{5'}$), 125.4 (q, ^1J = 270.0 Hz, CF_3), 127.1 (CH), 128.4 (C), 128.5 ($C_{2'}$, $C_{6'}$), 129.6 (CH), 130.2 (q, ^2J = 33.0 Hz, $C_{4'}$), 132.9 (CH), 135.4 (C), 139.5 (C), 144.2 ($C_{1'}$), 161.7 (CO), 165.9 (CO); ESI-MS *m/z* 322 (M + H)$^+$ (25), 294 (60), 276 (100). Anal. ($C_{16}H_{10}F_3NO_3$) C, H, N.

(xviii) 2-Hydroxy-7-phenylisoquinoline-1,3(2*H*,4*H*)-dione (6q): recrystallization solvent, ethanol; keto form (100%); yellow solid; 80% yield; mp 195 °C; ^{1}H NMR (DMSO-d_6) δ 4.27 (s, 2H, H_4), 7.20−7.56 (m, 4H, HAr), 7.70 (d, 2H, ^3J = 8.0 Hz, HAr), 7.93 (dd, 1H, ^3J = 8.0 Hz, ^4J = 2.0 Hz, H_6), 8.31 (d, 1H, ^4J = 2.0 Hz, H_8), 9.46 (s, 1H, OH); ^{13}C NMR (DMSO-d_6) δ 37.5 (C_4), 119.5 (C), 120.8 (2CH), 121.1 (CH), 121.7 (CH), 121.9 (CH), 122.8 (2CH), 125.7 (C), 126.3 (CH), 127.7 (C), 132.8 (C), 155.3 (CO), 159.5 (CO); ESI-MS *m/z* 254 (M + H)$^+$. Anal. ($C_{15}H_{11}NO_3$) C, H, N.

(xix) 2-Hydroxy-7-(4-hydroxyphenyl)isoquinoline-1,3(2*H*,4*H*)-dione (6r): treatment with boron tribromide (5 equiv); keto form (100%); orange solid; 60% yield; mp 195 °C; ^{1}H NMR (DMSO-d_6) δ 4.27 (s, 2H, H_4), 6.87 (d, 2H, ^3J = 8.5 Hz, HAr), 7.42 (d, 1H, ^3J = 8.0 Hz, H_5), 7.55 (d, 2H, ^3J = 8.5 Hz, HAr), 7.87 (dd, 1H, ^3J = 8.0 Hz, ^4J = 2.0 Hz, H_6), 8.15 (d, 1H, ^4J = 2.0 Hz, H_8), 9.46 (s, 1H, OH); ^{13}C NMR (DMSO-d_6) δ 36.5 (C_4), 116.2 (2CH), 127.2 (CH), 129.6 (CH), 130.7 (CH), 131.0 (C), 131.2 (2CH), 133.0 (C), 135.9 (C), 136.6 (C), 156.7 (CO), 160.2 (CO); ESI-MS *m/z* 270 (M + H)$^+$. Anal. ($C_{15}H_{11}NO_4$) C, H, N.

(xx) 7-(3,4-Dihydroxyphenyl)-2-hydroxyisoquinoline-1,3(2*H*,4*H*)-dione (6s): treatment with boron tribromide (6 equiv); keto form (100%); black solid; 57% yield; mp 178 °C; ^{1}H NMR (acetone-d_6) δ 4.26 (s, 2H, H_4), 6.95 (d, 1H, ^3J = 8.5 Hz, $H_{5'}$), 7.08 (dd, 1H, ^3J = 8.5 Hz, ^4J = 2.0 Hz, $H_{6'}$), 7.20 (d, 1H, ^4J = 2.0 Hz, $H_{2'}$), 7.47 (d, 1H, ^3J = 8.0 Hz, H_5), 7.86 (dd, 1H, ^3J = 8.0 Hz, ^4J = 2.0 Hz, H_6), 8.15 (s, 1H, OH), 8.19 (s, 1H, OH), 8.24 (d, 1H, ^4J = 2.0 Hz, H_8), 9.49 (s, 1H, OH); ^{13}C NMR (acetone-d_6) δ 30.9 (C_4), 108.3 (CH), 108.7 (C), 110.4 (CH), 113.0 (CH), 113.9 (C), 119.7 (CH), 120.3 (C), 122.7 (CH), 125.8 (CH), 127.0 (C), 134.9 ($C_{3'}$), 140.2 ($C_{4'}$), 155.6 (CO), 159.7 (CO); ESI-MS *m/z* 286 (M + H)$^+$. Anal. ($C_{15}H_{11}NO_5$) C, H, N.

Integrase Inhibition. To determine the susceptibility of the HIV-1 integrase enzyme to different compounds, we used an

enzyme-linked immunosorbent assay. This assay uses an oligonucleotide substrate in which one oligo (5′-ACTGCTAGAGATTTTCCACACTGACTAAAAGGGTC-3′) is labeled with biotin on the 3′ end and in which the other oligo is labeled with digoxigenin at the 5′ end. For the overall integration assay, the second 5′-digoxigenin-labeled oligo is 5′-GACCCTTTTAGTCAGTGTGGAAAATCTCTAGCA**GT**-3′. The integrase was diluted in 750 mM NaCl, 10 mM Tris (pH 7.6), 10% glycerol, 1 mM β-mercaptoethanol, and 0.1 mg/mL bovine serum albumin. To perform the reaction, 4 μL of diluted integrase (corresponds to a concentration of WT integrase[48] of 1.6 μM) and 4 μL of annealed oligos (7 nM) were added in a final reaction volume of 40 μL containing 10 mM $MgCl_2$, 5 mM DTT, 20 mM HEPES (pH 7.5), 5% PEG, and 15% DMSO. The reaction was carried out for 1 h at 37 °C. These reactions were followed by an immunosorbent assay on avidin-coated plates.[49] 3′-Processing and strand transfer assays were performed according to previously reported methods.[50]

In Vitro Anti-HIV and Drug Susceptibility Assays. The inhibitory effect of antiviral drugs on the HIV-1-induced cytopathic effect (CPE) in human lymphocyte MT-4 cell culture was determined by the MT-4/MTT assay.[51] This assay is based on the reduction of the yellow colored 3-(4,5-dimethylthiazol-2-yl)-2,5-diphenyltetrazolium bromide (MTT) by mitochondrial dehydrogenase of metabolically active cells to a blue formazan derivative, which can be measured spectrophotometrically. The 50% cell culture infective dose ($CCID_{50}$) of the HIV-1 (III_B) strain was determined by titration of the virus stock using MT-4 cells. For the drug susceptibility assays, MT-4 cells were infected with 100−300 $CCID_{50}$ of the virus stock in the presence of 5-fold serial dilutions of the antiviral drugs. The concentration of various compounds achieving 50% protection against the CPE of the different HIV strains, which is defined as the EC_{50}, was determined. In parallel, the 50% cytotoxic concentration (CC_{50}) was determined.

RT Assays. (i) RNase H Assay. The substrate for RNase H activity was prepared as previously described.[52] *E. coli* RNA polymerase used single-stranded calf thymus DNA as a template to synthesize complementary ^{3}H-labeled RNA. For RNase H activity, recombinant HIV-1 RT[53] (4.5 pmol) was incubated with the appropriate compound for 10 min at 37 °C in 20 μL. The components of the incubation mixture were added to reach a final concentration of 50 mM Tris-HCl (pH 8.0), 10 mM dithiothreitol, 6 mM $MgCl_2$, 80 mM KCl, and the labeled nucleic acid duplex (20000 cpm) in a final volume of 50 μL. After incubation for 10 min at 37 °C, the reaction was stopped by addition of 1 mL of cold 10% TCA containing 0.1 M sodium pyrophosphate. Samples were filtered on nitrocellulose filters and washed, and the radioactivity was determined.

(ii) DNA Polymerase Assay. Recombinant RT was incubated with the appropriate compound for 10 min at 37 °C in 20 μL. Then incubation was carried out at 37 °C for 10 min. The reaction mixture contained in a final volume of 0.05 mL 50 mM Tris-HCl (pH 8.0), 5 mM $MgCl_2$, 10 mM dithiothreitol, 100 mM KCl, 20 μg/mL poly(A)-oligo(dT), 0.5 μCi of [^{3}H]dTTP (56 Ci/mmol), 20 μM dTTP, and enzyme. Reactions were stopped by the addition of 1 mL of 10% cold trichloroacetic acid with 0.1 M sodium pyrophosphate. The precipitate was filtered through a nitrocellulose membrane washed with 2% trichloroacetic acid and dried, and the radioactivity was determined.

Molecular Modeling Study. Compounds **6a** and **6m** were sketched within Catalyst REF and minimized to their closest local energy minimum using a molecular mechanics approach. Poled conformations were generated for each molecule using the "Best" conformer generation option and an energy cutoff of 10 kcal/mol. For the estimation of the activity, we used a previously developed HypoGen pharmacophore model[38] and the BestEst option of the ViewHypothesis Workbench in Catalyst (Catalyst version 4.9, Accelrys Inc., San Diego, CA).

UV−Vis Experiments. The variation of the absorption was measured at 302.5 and 365.5 nm. For the stoichiometry determination, methanolic ligand and magnesium acetate solutions (0.5−1.0 mM) were prepared. In a typical Job plot experiment, x mL of a ligand solution was mixed with $1 - x$ mL of an equally concentrated magnesium solution, and the same amount of ligand was put into the reference cuvette. The absorbance was measured at the characteristic wavelength, and similar experiments were conducted by varying the ligand volumic fraction x. The absorbances were plotted against the ligand volumic fraction x, and the complex stoichiometry was estimated at the absorbance maximum. This procedure was repeated for different concentrations and at the two wavelengths until a consistent set of values was obtained. For the determination of the association constant, a typical experiment consisted of mixing x mL of a ligand solution and $1 - x$ mL of a differently concentrated magnesium solution. The same amount of ligand was put into the reference cuvette. For a 1/1 complex, the association constant K was given by

$$K = (p - 1)(1 - 2x)/\{[\mathrm{Mg}][(1 + p)x - 1]^2\}$$

where x and [Mg] are the ligand volumic fraction and the magnesium concentration, respectively, and p is the [ligand]/[Mg] ratio.

Acknowledgment. This work was financially supported by grants from la Région Nord Pas-de-Calais, le Centre National de la Recherche Scientifique (CNRS), l′Agence Nationale de la Recherche contre le Sida (ANRS), and the European Commission (LSHB-CT-2003-503480). The European TRIoH Consortium is gratefully acknowledged. The Mass Spectrometry facility used in this study was funded by the European Community (FEDER), the Région Nord-Pas de Calais (France), the CNRS, and the Université des Sciences et Technologies de Lille. We are grateful to Martine Michiels, Nam Joo Vanderveken, and Barbara Van Remoortel for excellent technical assistance.

Supporting Information Available: Additional chemical and biological information. This material is available free of charge via the Internet at http://pubs.acs.org.

References

(1) Goldgur, Y.; Dyda, F.; Hickman, A. B.; Jenkins, T. M.; Craigie, R.; Davies, D. R. Three new structures of the core domain of HIV-1 integrase: An active site that binds magnesium. *Proc. Natl. Acad. Sci. U.S.A.* **1998**, *95*, 9150–9154.
(2) Maignan, S.; Guilloteau, J. P.; Zhou-Liu, Q.; Clément-Mella, C.; Mikol, V. Crystal structures of the catalytic domain of HIV-1 integrase free and complexed with its metal cofactor: High level of similarity of the active site with other viral integrases. *J. Mol. Biol.* **1998**, *282*, 359–368.
(3) Makhija, M. T. Designing HIV integrase inhibitors: Shooting the last arrow. *Curr. Med. Chem.* **2006**, *13*, 2429–2441.
(4) Lataillade, M.; Kozal, M. J. The hunt for HIV-1 integrase inhibitors. *AIDS Patient Care STDS* **2006**, *20*, 489–501.
(5) Dayam, R.; Deng, J.; Neamati, N. HIV-1 integrase inhibitors: 2003−2004 update. *Med. Res. Rev.* **2006**, *26*, 271–309.
(6) Pommier, Y.; Johnson, A. A.; Marchand, C. Integrase inhibitors to treat HIV/AIDS. *Nat. Rev. Drug Discovery* **2005**, *4*, 236–248.
(7) Johnson, A. A.; Marchand, C.; Pommier, Y. HIV-1 integrase inhibitors: A decade of research and two drugs in clinical trial. *Curr. Top. Med. Chem.* **2004**, *4*, 1059–1077.
(8) Maurin, C.; Bailly, F.; Cotelle, P. Structure-activity relationships of HIV-1 integrase inhibitors: Enzyme-ligand interactions. *Curr. Med. Chem.* **2003**, *10*, 1795–1810.
(9) Cotelle, P. Patented HIV-1 integrase inhibitors (1998−2005). *Recent Patents Anti-Infect. Drug Discovery* **2006**, *1*, 1–15.
(10) Dejesus, E.; Berger, D.; Markowitz, M.; Cohen, C.; Hawkins, T.; Ruane, P.; Elion, R.; Farthing, C.; Zhong, C. L.; Cheng, A. K.; McColl, D.; Kearney, B. P. Antiviral activity, pharmacokinetics, and dose response of the HIV-1 integrase inhibitor GS-9137 (JTK-303) in treatment-naive and treatment-experienced patients. *J. Acquired Immune Defic. Syndr.* **2006**, *43*, 1–5.
(11) Grinsztejn, B.; Nguyen, B. Y.; Katlama, C.; Gatell, J. M.; Lazzarin, A.; Vittecoq, D.; Gonzalez, C. J.; Chen, J.; Harvey, C. M.; Isaacs,

R. D. Safety and efficacy of the HIV-1 integrase inhibitor raltegravir (MK-0518) in treatment-experienced patients with multidrug-resistant virus: A phase II randomised controlled trial. *Lancet* **2007**, *369*, 1261–1269.

(12) Markowitz, M.; Morales-Ramires, J. O.; Nguyen, B. Y.; Kovacs, C. M.; Steigbigel, R. T.; Cooper, D. A.; Liporace, R.; Schwartz, R.; Isaacs, R.; Gilde, L. R.; Wenning, L.; Zhao, J.; Teppler, H. Antiretroviral activity, pharmacokinetics, and tolerability of MK-0518, a novel inhibitor of HIV-1 integrase, dosed as monotherapy for 10 days in treatment-naive HIV-1-infected individuals. *J. Acquired Immune Defic. Syndr.* **2006**, *43*, 509–515.

(13) Freed, E. O.; Martin, M. A. HIVs and their replication. In *Fields Virology*; Knipe, D., Howley, P., Eds.; Lippincott Williams & Wilkins: Philadelphia, 2001; pp 1971−2042.

(14) Telesnitsky, A.; Goff, S. P. Reverse transcriptase and the generation of viral DNA. In *Retroviruses*; Coffin, J. M., Hughes, S. H., Varmus, H. E., Eds.; Cold Spring Harbor Laboratory Press: Plainview, NY, 1997; pp 121−160.

(15) Jacobo-Molina, A.; Ding, J.; Nanni, R. G.; Clark, A. D., Jr.; Lu, X.; Tantillo, C.; Williams, R. L.; Kamer, G.; Ferris, A. L.; Clark, P.; Hizi, A.; Hughes, S. H.; Arnold, E. Crystal structure of human immunodeficiency virus type 1 reverse transcriptase complexed with double-stranded DNA at 3.0 Å resolution shows bent DNA. *Proc. Natl. Acad. Sci. U.S.A.* **1993**, *90*, 6320–6324.

(16) Huang, H.; Chopra, R.; Verdine, G. L.; Harrison, S. C. Structure of a covalently trapped catalytic complex of HIV-1 reverse transcriptase: Implications for drug resistance. *Science* **1998**, *282*, 1669–1675.

(17) (a) Yang, W.; Steitz, T. A. Recombining the structures of HIV integrase, RuvC and RNase H. *Structure* **1995**, *3*, 131–134. (b) Haren, L.; Ton-Hoang, B.; Chandler, M. Integrating DNA: Transposases and retroviral integrases. *Annu. Rev. Microbiol.* **1999**, *53*, 245–281.

(18) Andréola, M. L. Closely related antiretroviral agents as inhibitors of two HIV-1 enzymes, ribonuclease H and integrase: "Killing two birds with one stone". *Curr. Pharm. Des.* **2004**, *10*, 3713–3723.

(19) Yang, W.; Hendrickson, W. A.; Crouch, R. J.; Satow, Y. Structure of ribonuclease H phased at 2 Å resolution by MAD analysis of the selenomethionyl protein. *Science* **1990**, *249*, 1398–1405.

(20) Davies, J. F., II; Hostomska, Z.; Hostomsky, Z.; Jordan, S. R.; Matthews, D. A. Crystal structure of the ribonuclease H domain of HIV-1 reverse transcriptase. *Science* **1991**, *252*, 88–95.

(21) Kaushik, N.; Rege, N.; Yadav, P. N.; Sarafianos, S. G.; Modak, M. J.; Pandey, V. N. Biochemical analysis of catalytically crucial aspartate mutants of human immunodeficiency virus type 1 reverse transcriptase. *Biochemistry* **1996**, *35*, 11536–11546.

(22) Patel, H. P.; Jacobo-Molina, A.; Ding, J.; Tantillo, C.; Clark, A. D.; Raag, R.; Nanni, R. G.; Hughes, S. H.; Arnold, E. Insights into DNA polymerisation mechanisms from structure and function analysis of HIV-1 reverse transcriptase. *Biochemistry* **1995**, *34*, 5351–5363.

(23) Shaw-Reid, C. A.; Munshi, V.; Graham, P.; Wolfe, A.; Witmer, M.; Danzeisen, R.; Olsen, D. B.; Carroll, S. S.; Embrey, M.; Wai, J. S.; Miller, M. D.; Cole, J. L.; Hazuda, D. J. Inhibition of HIV-1 ribonuclease H by a novel diketo acid, 4-[5-(benzoylamino)thien-2-y]-2,4-dioxobutanoic acid. *J. Biol. Chem.* **2003**, *278*, 2777–2780.

(24) Tramontano, E.; Esposito, F.; Badas, R.; Di Santo, R.; Costi, R.; La Colla, P. 6-[1-(4-Fluorophenyl)methyl-1H-pyrrol-2-yl)]-2,4-dioxo-5-hexenoic acid ethyl ester a novel diketo acid derivative which selectively inhibits the HIV-1 viral replication in cell culture and the ribonuclease H activity in vitro. *Antiviral Res.* **2005**, *65*, 117–124.

(25) de Soultrait, V.; Lozach, P.; Altmeyer, R.; Tarrago-Litvak, L.; Litvak, S.; Andréola, M. L. DNA aptamers derivated from HIV-1 RNase H inhibitors are strong anti-integrase agents. *J. Mol. Biol.* **2002**, *324*, 195–203.

(26) Didierjean, J.; Isel, C.; Querré, F.; Mouscadet, J. F.; Aubertin, A. M.; Valnot, J. Y.; Piettre, S. R.; Marquet, R. Inhibition of human immunodeficiency virus type 1 reverse transcriptase, RNase H, and integrase activities by hydroxytropolones. *Antimicrob. Agents Chemother.* **2005**, *49*, 4884–4894.

(27) Budihas, S.; Gorshkova, I.; Gaidamakov, S.; Wamiru, A.; Bona, M.; Parniak, M.; Crouch, R.; McMahon, J.; Beutler, J.; Le Grice, S. Selective inhibition of HIV-1 reverse transcriptase-associated ribonuclease H activity by hydroxylated tropolones. *Nucleic Acids Res.* **2005**, *33*, 1249–1256.

(28) Semenova, E. A.; Johnson, A. A.; Marchand, C.; Davis, D. A.; Yarchoan, R.; Pommier, Y. Preferential inhibition of the magnesium-dependent strand transfer reaction of HIV-1 integrase by α-hydroxytropolones. *Mol. Pharmacol.* **2006**, *69*, 1454–1460.

(29) Marchand, C.; Beutler, J. A.; Wamiru, A.; Budihas, S.; Möllmann, U.; Heinisch, L.; Mellors, J. W.; Le Grice, S. F.; Pommier, Y. Madurahydroxylactone derivatives as dual inhibitors of human immunodeficiency virus type 1 integrase and RNase H. *Antimicrob. Agents Chemother.* **2008**, *52*, 361–364.

(30) Hang, J. Q.; Rajendran, S.; Yang, Y.; Li, Y.; Wong Kai In, P.; Overton, H.; Parkes, K. E. B.; Cammack, N.; Martin, J. A.; Klumpp, K. Activity of the isolated HIV RNase H domain and specific inhibition by N-hydroxyimides. *Biochem. Biophys. Res. Commun.* **2004**, *317*, 321–329.

(31) Parkes, K. E. B.; Ermert, P.; Fassler, J.; Ives, J.; Martin, J. A.; Merrett, J. H.; Obrecht, D.; Williams, G.; Klumpp, K. Use of a pharmacophore model to discover a new class of influenza endonuclease inhibitors. *J. Med. Chem.* **2003**, *46*, 1153–1164.

(32) Klumpp, K.; Hang, J. Q.; Rajendran, S.; Yang, Y.; Derosier, A.; Wong Kai In, P.; Overton, H.; Parkes, K. E. B.; Cammack, N.; Martin, J. A. Two-metal-ion mechanism of RNA cleavage by HIV RNase H and mechanism based design of selective HIV RNase H inhibitors. *Nucleic Acids Res.* **2003**, *31*, 6852–6859.

(33) Ames, D. E.; Grey, T. F. N-Hydroxyimides. II. *J. Chem. Soc.* **1955**, *351*, 3518–3521.

(34) Horeau, A.; Jacques, J. Isocoumarins. *Bull. Soc. Chim. Fr.* **1948**, 53–59.

(35) Ungnade, H.; Nightingale, D.; French, H. The synthesis of 7-methoxyisoquinolone. *J. Org. Chem.* **1945**, *10*, 533–536.

(36) Geffken, D. Zur cycliesierung von salicylsäureamiden und Salicylhydroxamsäuren von 1,1′-carbonyldiimidazol. *Liebigs Ann. Chem.* **1981**, 1513–1514.

(37) Sechi, M.; Bacchi, A.; Carcelli, M.; Compari, C.; Duce, E.; Fisicaro, E.; Rogolino, D.; Gates, P.; Derudas, M.; Al-Mawsawi, L. Q.; Neamati, N. From ligand to complexes: Inhibition of human immunodeficiency virus type 1 integrase by β-diketo acid metal complexes. *J. Med. Chem.* **2006**, *49*, 4248–4260.

(38) Barreca, M. L.; Ferro, S.; Rao, A.; De Luca, L.; Zappala, M.; Monforte, A. M.; Debyser, Z.; Witvrouw, M.; Chimirri, A. Pharmacophore-based design of HIV-1 integrase strand-transfer inhibitors. *J. Med. Chem.* **2005**, *48*, 7084–7088.

(39) Hazuda, D. J.; Felock, P.; Witmer, M.; Wolfe, A.; Stillmock, K.; Grobler, J. A.; Espeseth, A.; Gabryelski, L.; Schleif, W.; Blau, C.; Miller, M. D. Inhibitors of strand transfer that prevent integration and inhibit HIV-1 replication in cells. *Science* **2000**, *287*, 646–650.

(40) Grobler, J. A.; Stillmock, K.; Binghua, H.; Witmer, M.; Felock, P.; Espeseth, A. S.; Wolfe, A.; Egbertson, M.; Bourgeois, M.; Melamed, J.; Wai, J. S.; Young, S.; Vacca, J.; Hazuda, D. J. Diketo acid inhibitor mechanism and integrase: Implications for metal binding in the active site of phosphotransferase enzymes. *Proc. Natl. Acad. Sci. U.S.A.* **2002**, *99*, 6661–6666.

(41) Rosemond, M. J.; St John-Williams, L.; Yamaguchi, T.; Fujishita, T.; Walsh, J. S. Enzymology of a carbonyl reduction clearance pathway for the HIV integrase inhibitor, S-1360: Role of human liver cytosolic aldo-keto reductases. *Chem.-Biol. Interact.* **2004**, *147*, 129–139.

(42) Deng, J.; Dayam, R.; Al-Mawsawi, L. Q.; Neamati, N. Design of second generation HIV-1 integrase inhibitors. *Curr. Pharm. Des.* **2007**, *13*, 129–141.

(43) Billich, A. S-1360 Shionogi-GlaxoSmithKline. *Curr. Opin. Invest. Drugs* **2003**, *4*, 206–209.

(44) Cooper, D.; Gatell, J.; Rockstroh, J.; Katlama, C.; Yeni, P.; Lazzarin, A.; Chen, J.; Isaacs, R.; Teppler, H.; Nguyen, B. (for the BENCHMRK-Study Group)Results of BENCHMRK-1, a Phase III Study Evaluating the Efficacy and Safety of MK-0518, a Novel HIV-1 Integrase Inhibitor, in Patients with Triple-Class Resistant Virus. 14th Conference on Retroviruses and Opportunistic Infections, Los Angeles, CA, February 25−28, 2007.

(45) Wang, Z.; Bennett, E. M.; Wilson, D. J.; Salomon, C.; Vince, R. Rationally designed dual inhibitors of HIV-1 reverse transcriptase and integrase. *J. Med. Chem.* **2007**, *50*, 3416–3419.

(46) Sato, M.; Motomura, T.; Aramaki, H.; Matsuda, T.; Yamashita, M.; Ito, Y.; Kawakami, H.; Matsuzaki, Y.; Watanabe, W.; Yamataka, K.; Ikeda, S.; Kodama, E.; Matsuoka, M.; Shinkai, H. Novel HIV-1 integrase inhibitors derived from quinolone antibiotics. *J. Med. Chem.* **2006**, *49*, 1506–1508.

(47) De Luca, L.; Barreca, M. L.; Ferro, S.; Iraci, N.; Michiels, M.; Christ, F.; Debyser, Z.; Witvrouw, M.; Chimirri, A. A refined pharmacophore model for HIV-1 integrase inhibitors: Optimisation of potency in the 1H-benzylindole series. *Bioorg. Med. Chem. Lett.* **2008**, *18*, 2891–2895.

(48) Debyser, Z.; Cherepanov, P.; Pluymers, W.; De Clercq, E. Assays for the evaluation of HIV-1 integrase inhibitors. *Methods Mol. Biol.* **2001**, *160*, 139–155.

(49) Hwang, Y.; Rhodes, D.; Bushman, F. Rapid microtiter assays for poxvirus topoisomerase, mammalian type IB topoisomerase and HIV-1 integrase: Application to inhibitor isolation. *Nucleic Acids Res.* **2000**, *28*, 4884–4892.

(50) Busschots, K.; Voet, A.; De Mayer, M.; Rain, J. C.; Emiliani, S.; Benarous, R.; Desender, L.; Debyser, Z.; Christ, F. Identification of the LEDGF/p75 binding site in HIV-1 integrase. *J. Mol. Biol.* **2007**, *365*, 1480–1492.

(51) Pauwels, R.; Balzarini, J.; Baba, M.; Snoeck, R.; Schols, D.; Herdewijn, P.; Desmyter, J.; De Clercq, E. Rapid and automated tetrazolium-based colorimetric assay for the detection of anti-HIV compounds. *J. Virol. Methods* **1988**, *20*, 309–321.
(52) Moelling, K.; Schulze, T.; Diringer, H. Inhibition of human immunodeficiency virus type 1 RNase H by polysulfated polyanions. *J. Virol.* **1989**, *63*, 5489–5491.
(53) Dufour, E.; Reinbolt, J.; Castroviejo, M.; Ehresmann, B.; Litvak, S.; Tarrago-Litvak, L.; Andreola, M. L. Cross-linking localization of a HIV-1 reverse transcriptase peptide involved in the binding of primer tRNALys3. *J. Mol. Biol.* **1999**, *285*, 1339–1346.

JM8007085